Juan Manuel Calleja Vázquez

ACOMEN - Liège 2022:

Pressure-dependent multiscale stochastic simulations using a MFH model constructed from full-field SVE realizations

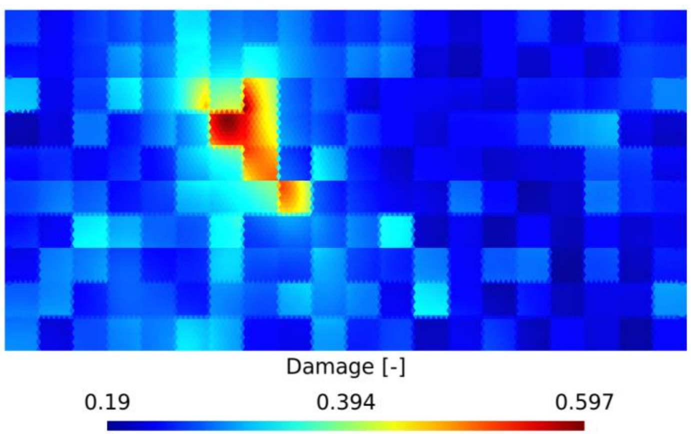

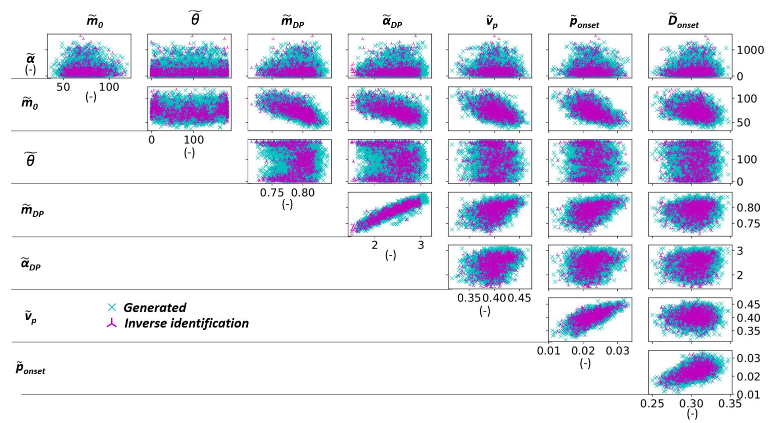

Motivation

- A look into the microstructure:
  - Non determinisms affect the SVE response → Each SVE has a different behavior
    - Geometrical
    - Fibre-matrix bonding
    - …

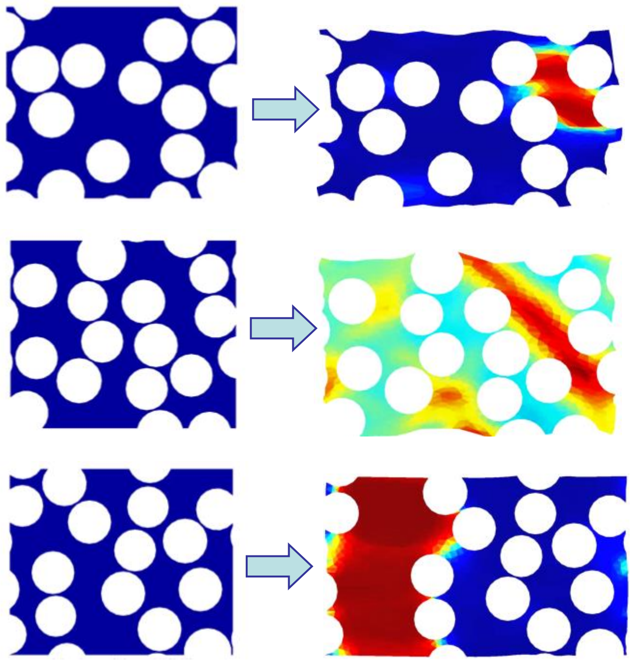

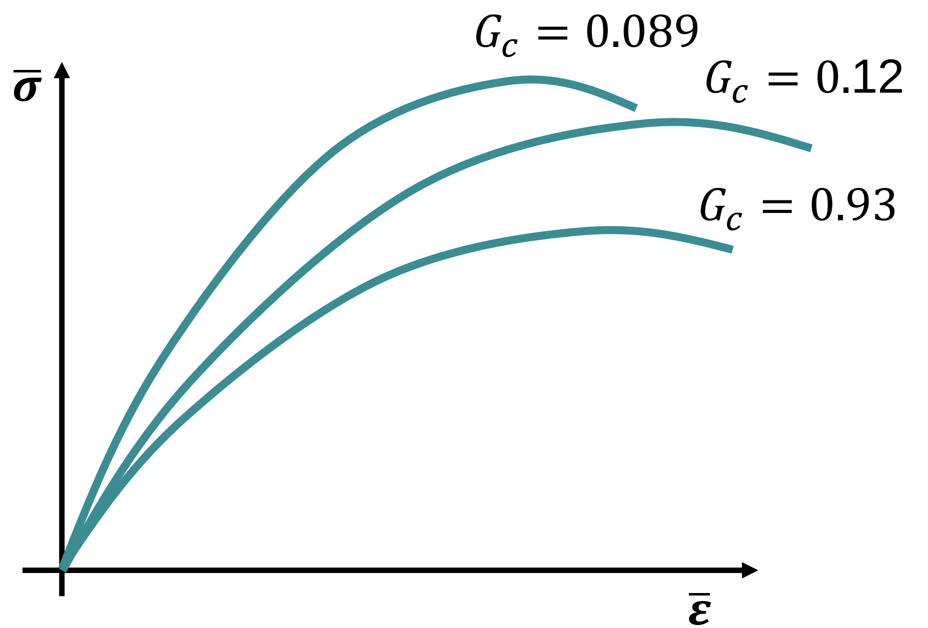

Motivation

- A look into the microstructure:
  - Need of a stochastic model in order to scale these uncertainties to the macroscale
  - Efficient model for the simulation is needed
    - Full-Field macro-scale simulations are prohibitive
      →High computational cost

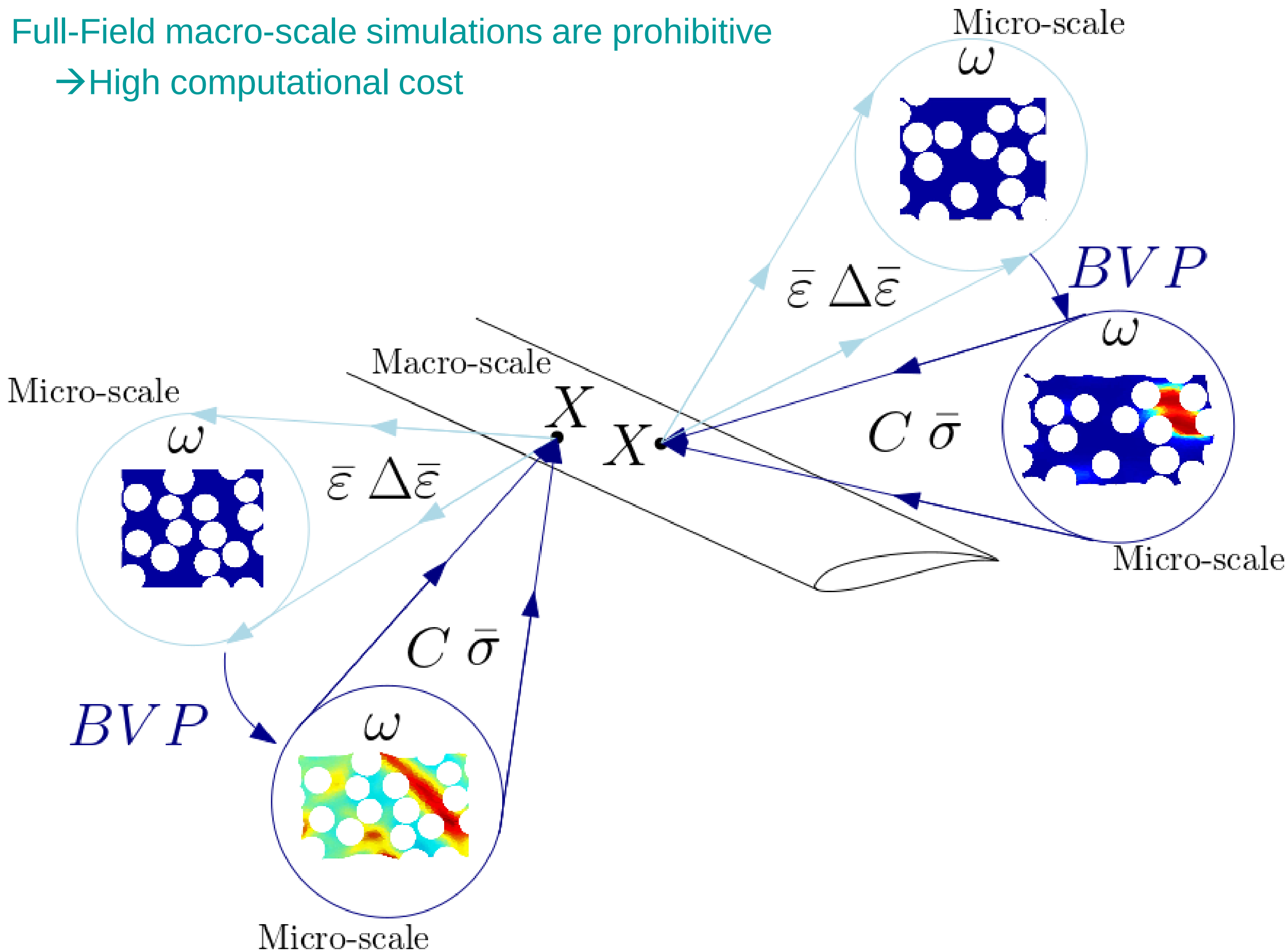

Methodology Overview: Stochastic MF-ROM

- Methodology scheme: From SEM images to efficient stochastic simulations

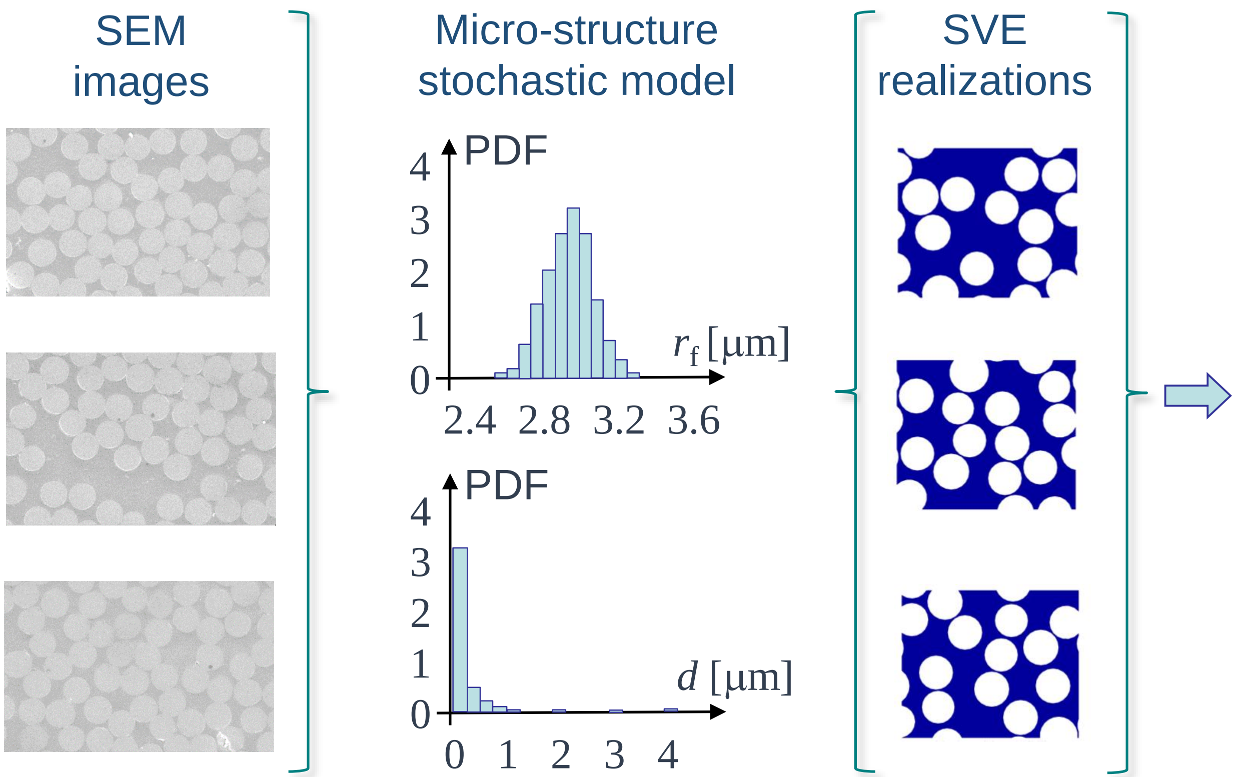

- Damaged elastic tensor $\bar{\boldsymbol{C}}^{elD}$
- $\bar{\varepsilon} - \bar{\sigma}$ evolution
- Energy release rate (G_c)
- Fiber volume fraction

Methodology Overview: Stochastic MF-ROM

- Methodology scheme: From SEM images to efficient stochastic simulations

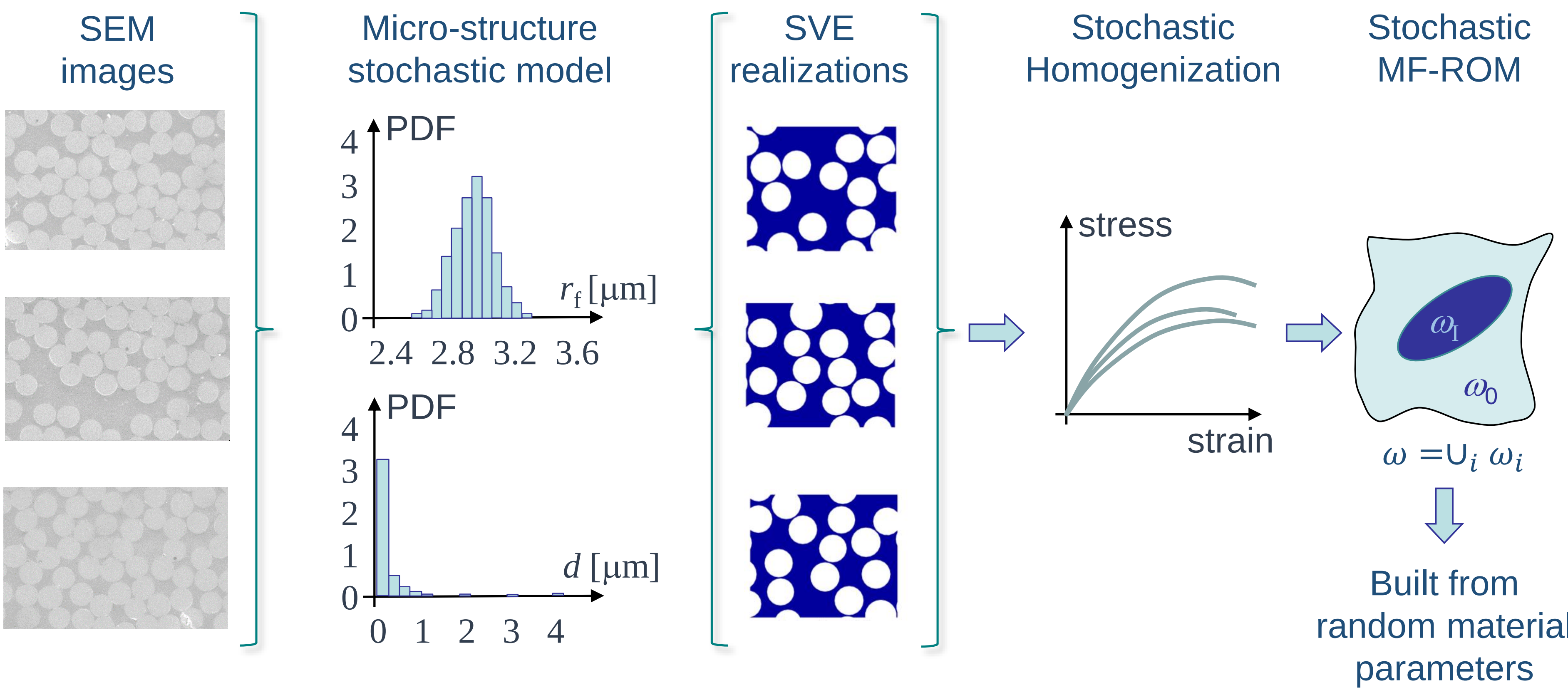

Full-Field Realizations: Large Strain Matrix Model

- UD Composites with RTM6 epoxy matrix
  - Full-field simulations performed with identified matrix material behaviors
    - Hyperelastic viscoelastic-viscoplastic constitutive model enhanced by a multi-mechanism non-local damage model
- Capable of accurately represent the behavior of the high crosslinked epoxy
- Represents the epoxy behavior up to its complete failure thanks to G_c calibration after the localization onset

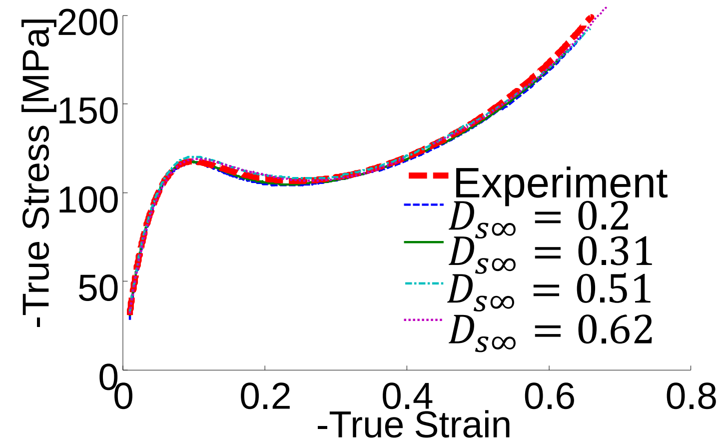

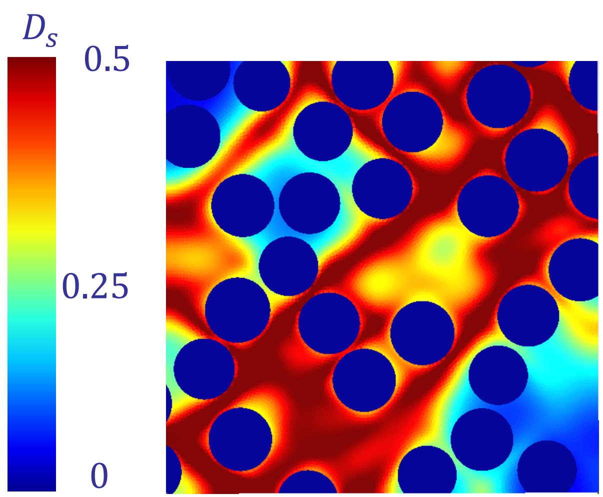

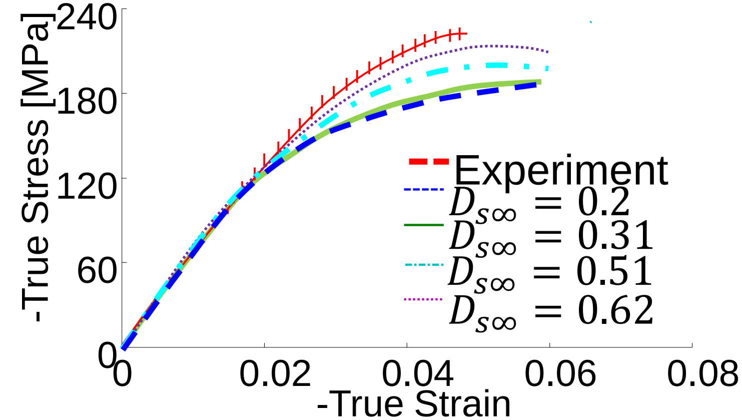

V.-D. Nguyen, L. Wu, L. Noels, A micro-mechanical model of reinforced polymer failure with length scale effects and predictive capabilities. Validation on carbon fiber reinforced high-crosslinked RTM6 epoxy resin

Incremental Secant MFH Scheme: Elasticity

- Elastic Stage

$$\bar{\boldsymbol{\varepsilon}} = v_0\boldsymbol{\varepsilon}_0 + v_I\boldsymbol{\varepsilon}_0$$

$$\bar{\boldsymbol{\sigma}} = v_0\boldsymbol{\sigma}_0 + v_I\boldsymbol{\sigma}_I$$

$$\boldsymbol{\varepsilon}_I = \boldsymbol{B}^{\epsilon}(I, \boldsymbol{C}_0, \boldsymbol{C}_I, v_I) : \boldsymbol{\varepsilon}_0$$

  - Where the Mori-Tanaka assumption is used for $\boldsymbol{B}^{\epsilon}$
  - How do we identify the elastic random vectors?

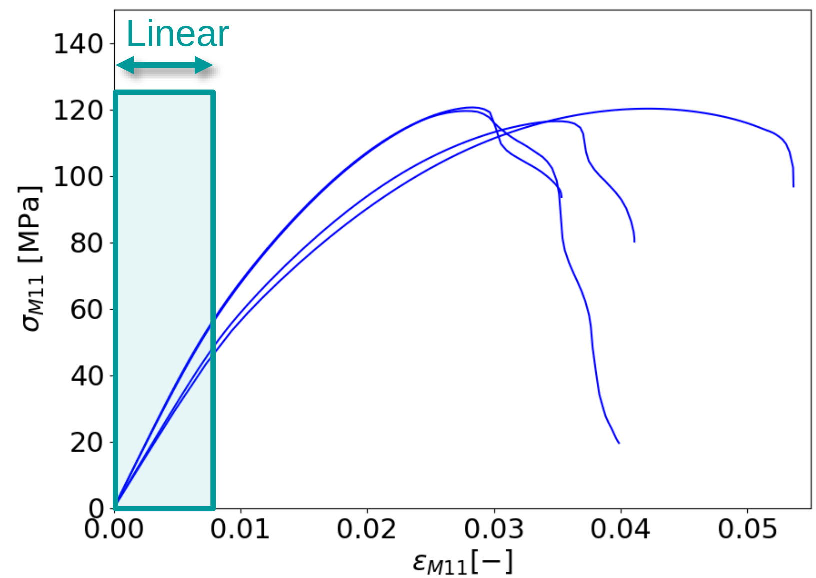

$$\min_{\tilde{I},\tilde{\theta},\tilde{E}_0,\tilde{v}_0} \left\| \left(\tilde{\bar{\boldsymbol{C}}}^{el}(\tilde{I}, \tilde{\theta}, \tilde{\boldsymbol{C}}_0^{el}(\tilde{E}_0, \tilde{v}_0)\right) - \bar{\boldsymbol{C}}^{el} \right\|$$

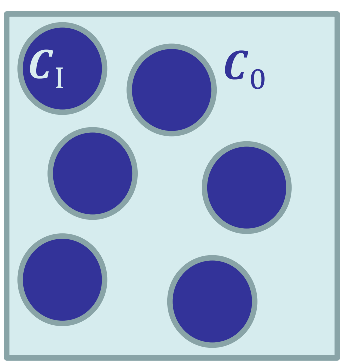

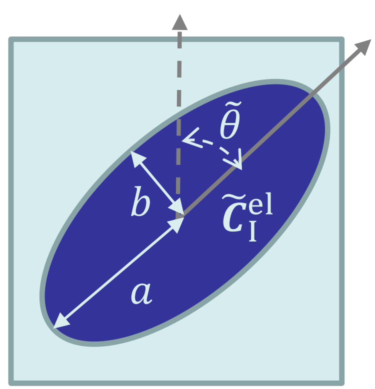

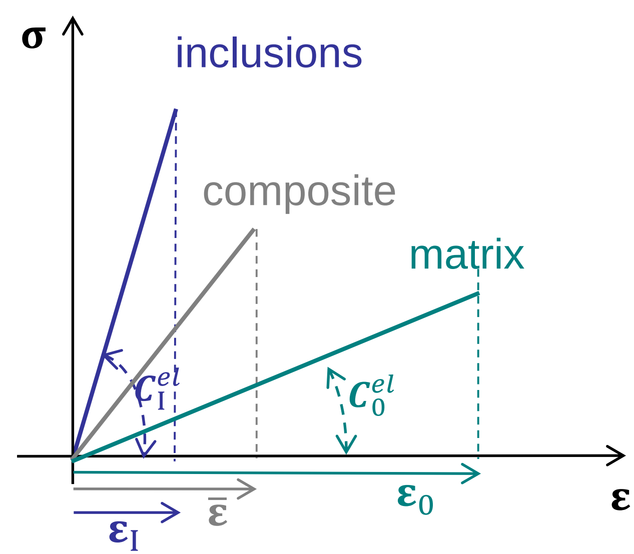

Incremental Secant MFH Scheme: Plasticity

- Damage-enhanced plasticity
  - Use of the incremental-secant MFH
  - Virtual elastic unloading from the previous state
    - Composite material unloaded to reach the stress-free state
    - Residual stress in components
    - Damage is taken into account in the matrix phase

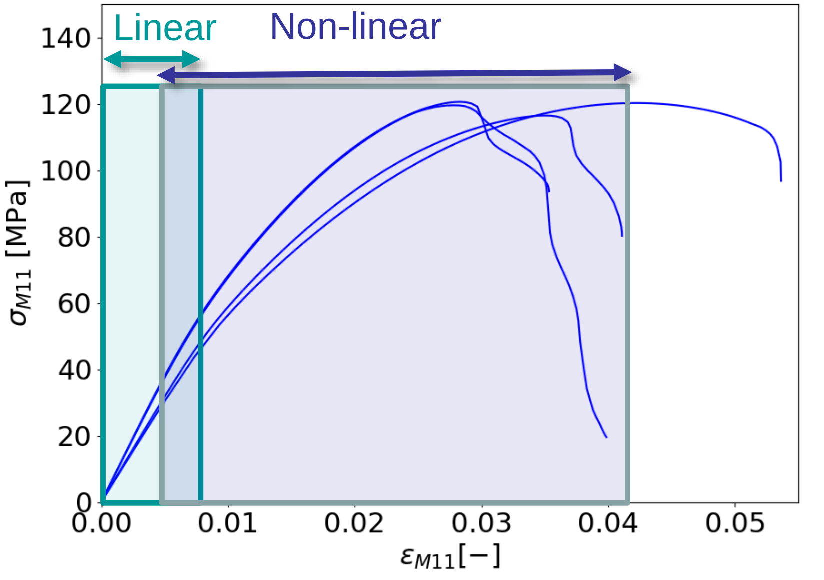

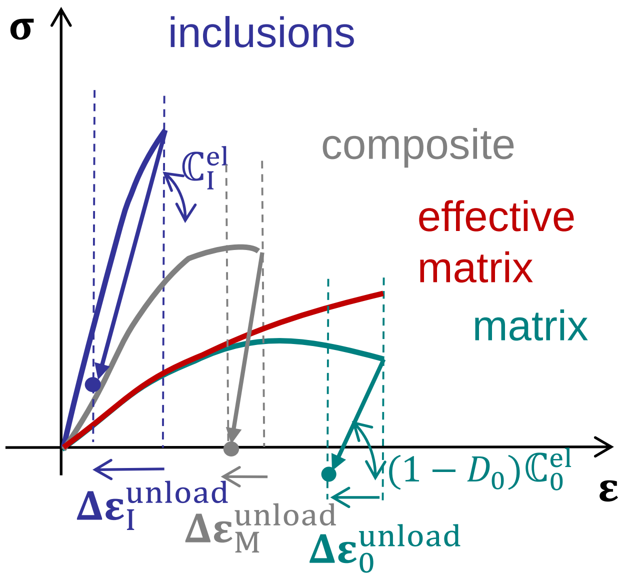

Incremental Secant MFH Scheme: Plasticity

- Damage-enhanced plasticity
  - Use of the incremental-secant MFH
  - Virtual elastic unloading from the previous state
    - Composite material unloaded to reach the stress-free state
    - Residual stress in components
    - Damage is taken into account in the matrix phase

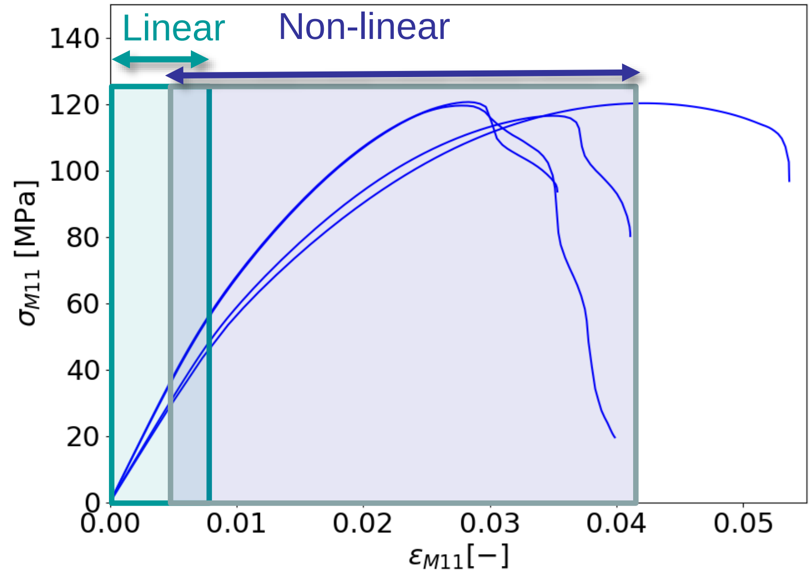

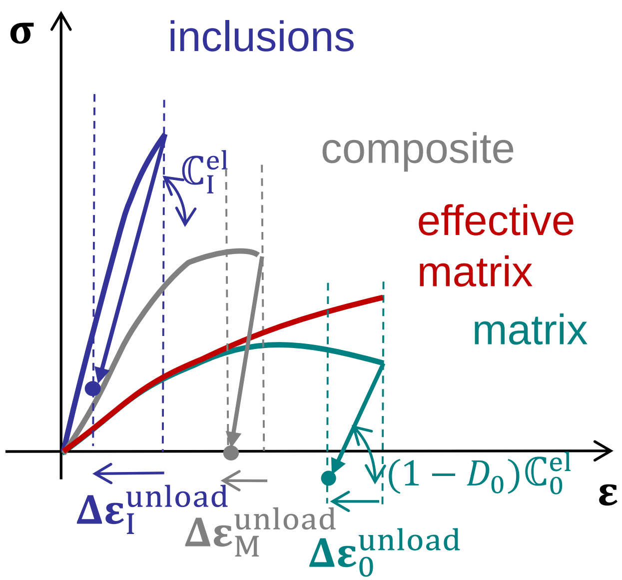

- $\widetilde{\boldsymbol{C}}_n^{elD}$ is extracted from full-field SVE realizations
  - $\widetilde{D}_{0_n}$ can be identified through a minimization process:

$$\min_{\widetilde{D}_{0_n}} \left\| \widetilde{\boldsymbol{C}}_n^{elD}\left(\widetilde{\boldsymbol{C}}_0^{elD}\left(\widetilde{D}_{0_n}\right)\right) - \overline{\boldsymbol{C}}_n^{elD} \right\|$$

  - $\widetilde{D}_0$ is then fitted through a dedicated damage evolution law

Incremental Secant MFH Scheme: Plasticity

- Damage-enhanced plasticity
  - Use of the incremental-secant MFH
  - Reload of the composite:
    - The composite material is reloaded to reach the next stress-strain state
    - Definition of the **LCC**
    - Damage is taken into account in the matrix phase

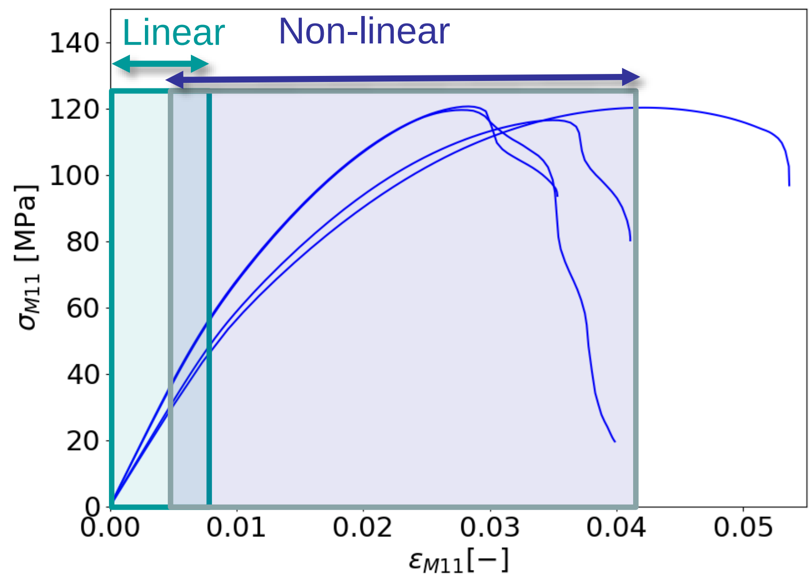

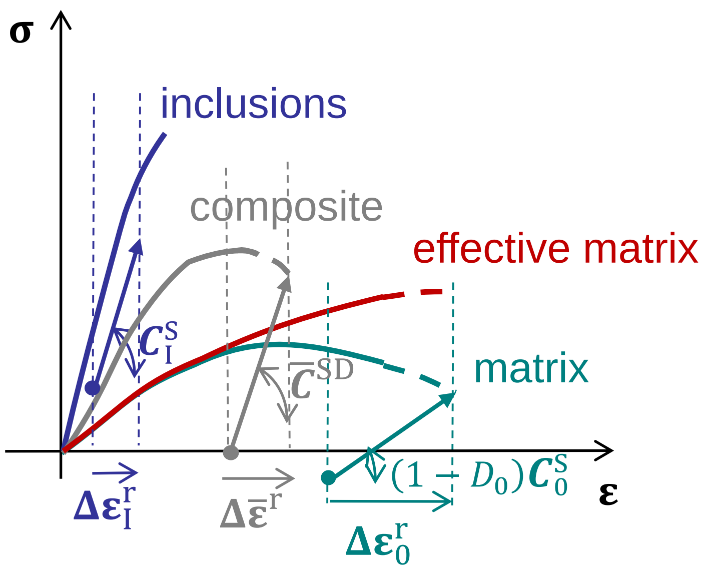

$$\Delta\overline{\boldsymbol{\varepsilon}}^r_{n+1} = v_0 \Delta\boldsymbol{\varepsilon}^r_{0_{n+1}} + v_I \Delta\boldsymbol{\varepsilon}^r_{I_{n+1}}$$

$$\overline{\boldsymbol{\sigma}}_{n+1} = v_0 \boldsymbol{\sigma}_{0_{n+1}} + v_I \boldsymbol{\sigma}_{I_{n+1}}$$

$$\Delta\boldsymbol{\varepsilon}^r_{I_{n+1}} = \boldsymbol{B}^{\epsilon} : \Delta\boldsymbol{\varepsilon}^r_{0_{n+1}}$$

- Incremental secant operator

$$\overline{\boldsymbol{\sigma}}_{n+1} = \overline{\boldsymbol{\sigma}}^{\boldsymbol{res}}{}_n + \overline{\boldsymbol{C}}^{SD}\left(I, (1-D_0)C_0^S, C_I^S, v_I\right) : \Delta\overline{\boldsymbol{\varepsilon}}^{\mathrm{r}}$$

LCC: Linear Comparison Composite

Incremental Secant MFH Scheme: Plasticity

- Enhanced Drucker-Prager yield function with non-associated plastic flow:

$$f(\hat{\boldsymbol{\sigma}}_{n+1}, p_n) = \frac{\left((\hat{\boldsymbol{\sigma}}_{n+1})^{eq}\right)^{\alpha}}{\sigma_c^{\alpha}} - 3\frac{m^{\alpha}-1}{(m+1)\sigma_c}\hat{\phi}_{n+1} - \frac{m^{\alpha}+m}{m+1} \leq 0$$

$$\boldsymbol{\sigma}_c = \boldsymbol{\sigma}_c^0 + R(p) \qquad \hat{\phi} = \frac{1}{3tr(\hat{\boldsymbol{\sigma}})}$$

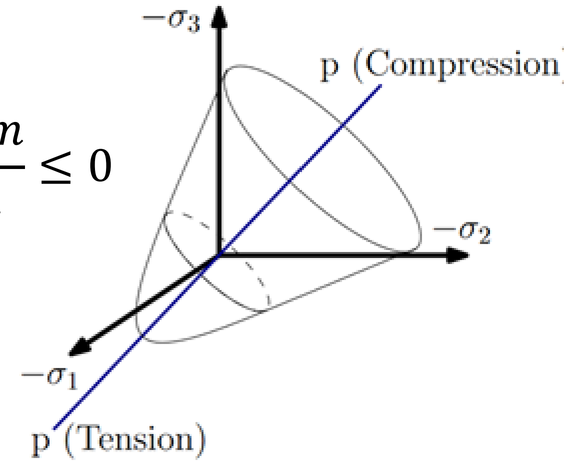

- C^{Sr} is found to be isotropic, being possible to write it in terms of μ_s^r and κ_s^r as:

$$\boldsymbol{C}^{Sr} = 3\kappa_s^r I^{vol} + 2\mu_s^r I^{dev}$$

  – Where

$$\kappa_s^r = \kappa_s^r(\kappa^{el}, \beta, \Gamma) \qquad \mu_s^r = \mu_s^r(\mu^{el}, \Gamma)$$

Stochastic MF-ROM: Parameter identification

- 16 random material parameters needed to describe the composite:

Already identified!

$$[\tilde{v}_I,\ \tilde{I},\ \tilde{\theta},\ \tilde{E}_0,\ \tilde{v},\ \tilde{\sigma}_y,\ \tilde{h}_0,\ \tilde{h}_1,\ \tilde{m}_0,\ \tilde{m},\ \tilde{v}_p,\ \tilde{\alpha},\ \tilde{p}_{onset},\ \tilde{D}_{onset},\ \tilde{\alpha}_{dam},\ \tilde{\beta}]$$

Elastic ($\tilde{v}_I, \tilde{I}, \tilde{\theta}, \tilde{E}_0, \tilde{v}, \tilde{\sigma}_y$) — Hardening ($\tilde{h}_0, \tilde{h}_1, \tilde{m}_0$) — Pressure ($\tilde{m}, \tilde{v}_p, \tilde{\alpha}$) — Damage ($\tilde{p}_{onset}, \tilde{D}_{onset}, \tilde{\alpha}_{dam}, \tilde{\beta}$)

- In order to fully describe the pressure-dependent model:
  - 3 full-field tests are needed for each SVE
  - Uniaxial tension, uniaxial compression and biaxial tests are used

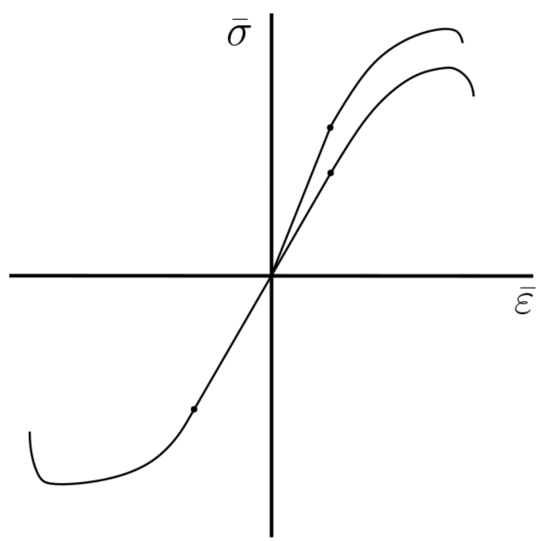

- Once the matrix stress-state is computed at the plasticity onset:
  - The accumulated plastic strain is supposed to be zero at this state
  - Solving the yield surface for the 3 tests allows to obtain the 3 parameters involved in its definition
    - $\tilde{\sigma}_y, \tilde{m}, \tilde{\alpha}$

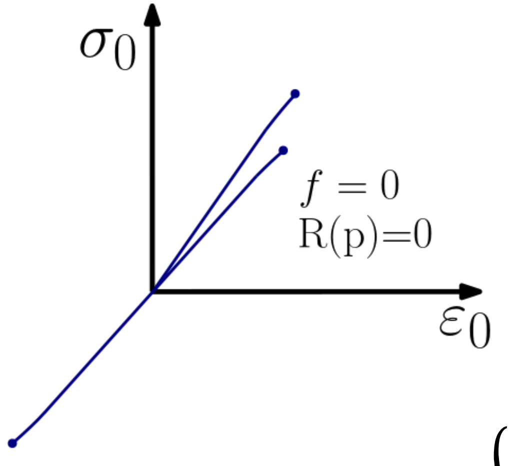

$$\min_{\alpha, m, \sigma_y} \left\{ \left\| \sum f(\alpha, m, \sigma_y) \right\| \right\}$$

  - Only one of the tests is needed for the remaining of the identification process
    - Uniaxial tension is used

- The matrix secant tensor is optimized at each step
  - The bulk and shear moduli remain the only unknown in its definition

$$\min_{\tilde{\mu}_s^{Dr};\tilde{\kappa}_s^{Dr}} \left\{ \left\| \tilde{\bar{\boldsymbol{C}}}^{SD}\left(\tilde{\boldsymbol{C}}_0^{SD}\left(\tilde{\mu}_s^{Dr};\tilde{\kappa}_s^{Dr}\right)\right):\Delta\bar{\boldsymbol{\varepsilon}}_n^r - \bar{\boldsymbol{\sigma}}_{n+1} \right\| \right\}$$

$$\mu_s^r = \mu_s^r(\mu^{el},\Gamma) \qquad \kappa_s^r = \kappa_s^r(\kappa^{el},\beta,\Gamma)$$

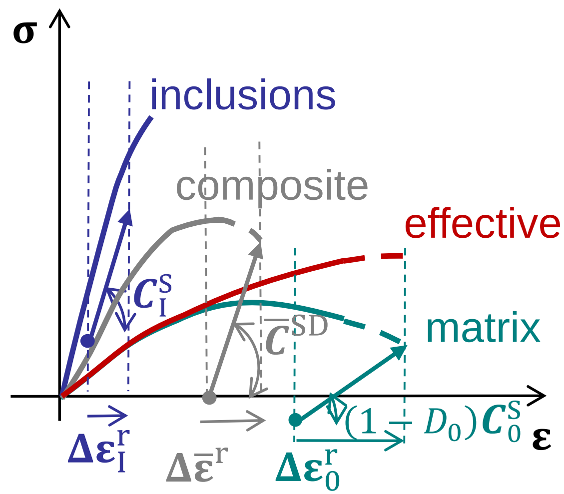

- The plastic multiplier allows then to compute the plastic strain evolution at each iteration

Stochastic MF-ROM: Parameter identification

- With $\tilde{\sigma}_y$,$\tilde{m}$ and $\tilde{\alpha}$ identified, $\tilde{p}_{0_n}$ and σ_{0_n} computed:
  - R_n remains the only unknown in the yield surface definition
  - During plasticity $f = 0$. R_n can be identified by the minimization problem:

$$\min_{R_n}\{\| f_n(R_n) \|\}$$

- A curve fitting process is used to identify the dedicated linear exponential hardening law parameters: $\tilde{h}_0$, $\tilde{h}_1$, $\tilde{m}_0$

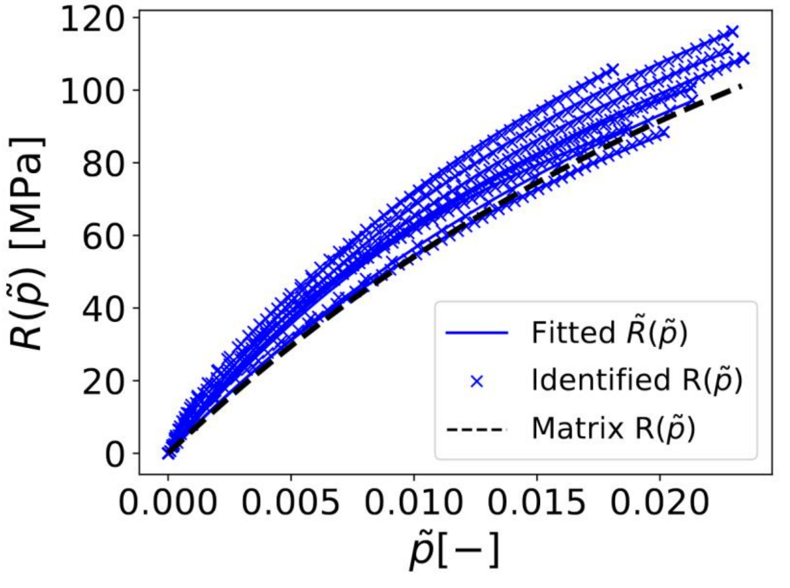

- Failure stage
  - Last stage in the MFH inverse analysis
    - Failure → Loss of size objectivity
    - Use of the energy release rate G_c as quantity that allows to recover the size objectivity
  - L >> l ; W << l cylinder to obtain MFH non-dimensional G_c
  - Optimization problem to recover SVE Gc value

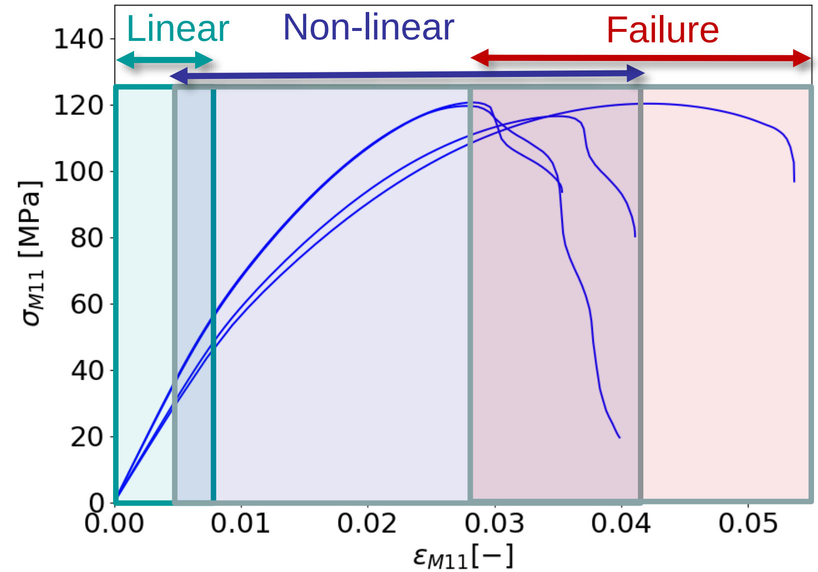

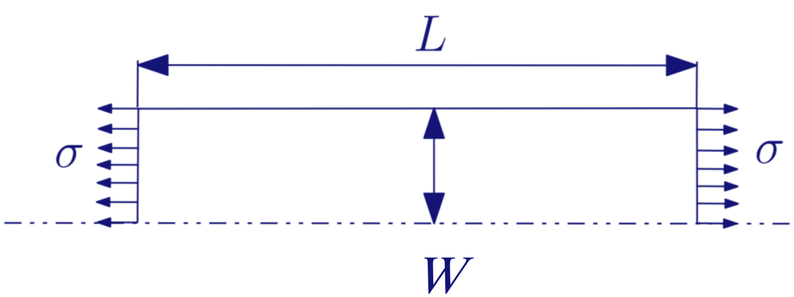

$$G_c = \frac{\mathcal{D}_{V_0}^{end} - \mathcal{D}_{V_0}^{loc}}{A_0}$$

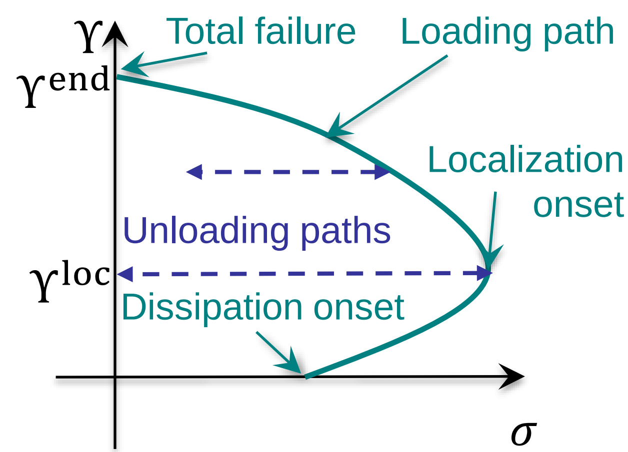

Stochastic MF-ROM

- Parameters are identified for 1050 SVE
- New data is generated using a Markov chain Monte Carlo (MCMC) process in order to obtain proper random fields

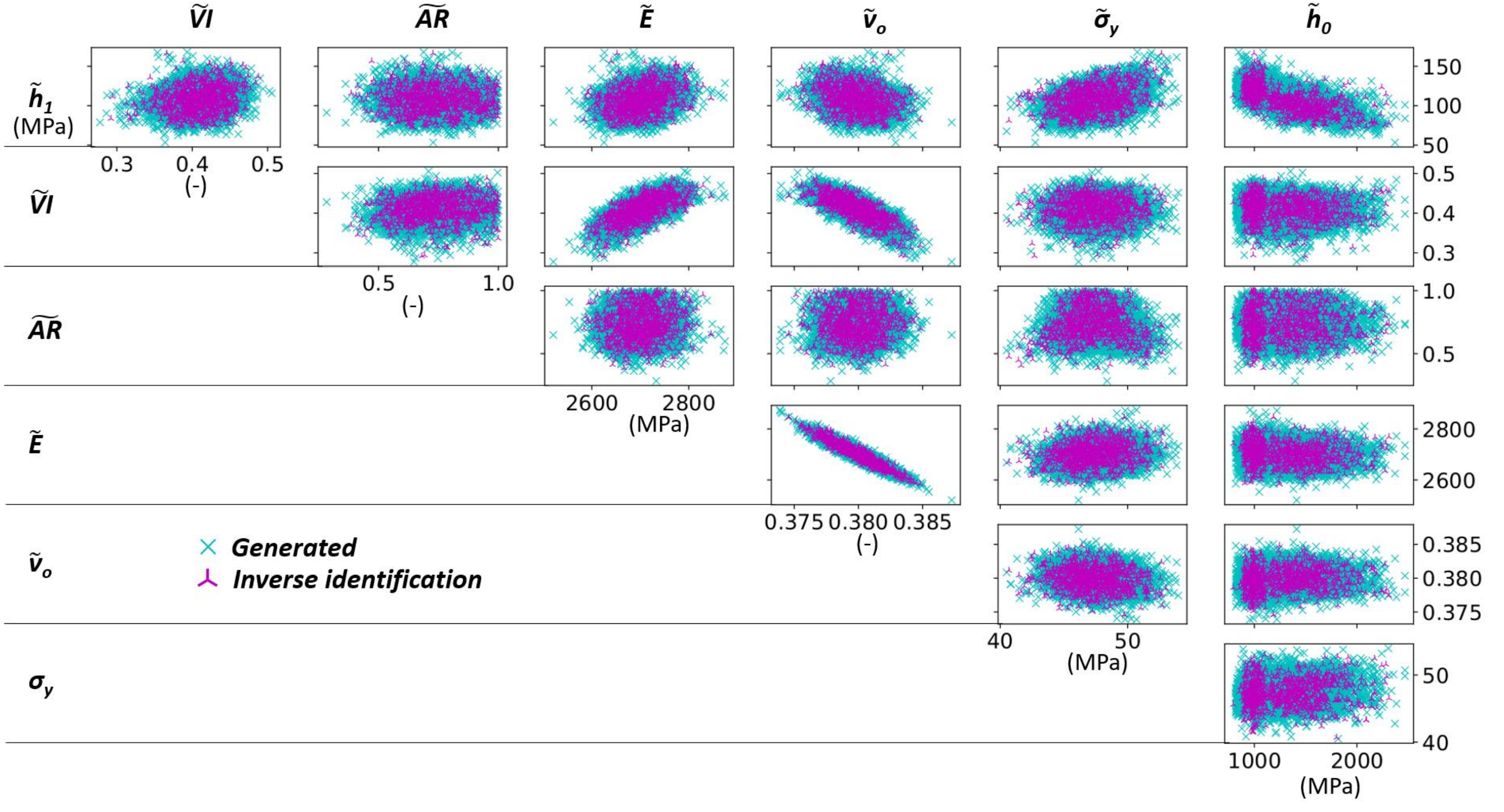

Stochastic MF-ROM

- Parameters are identified for 1050 SVE
- New data is generated using a Markov chain Monte Carlo (MCMC) process in order to obtain proper random fields

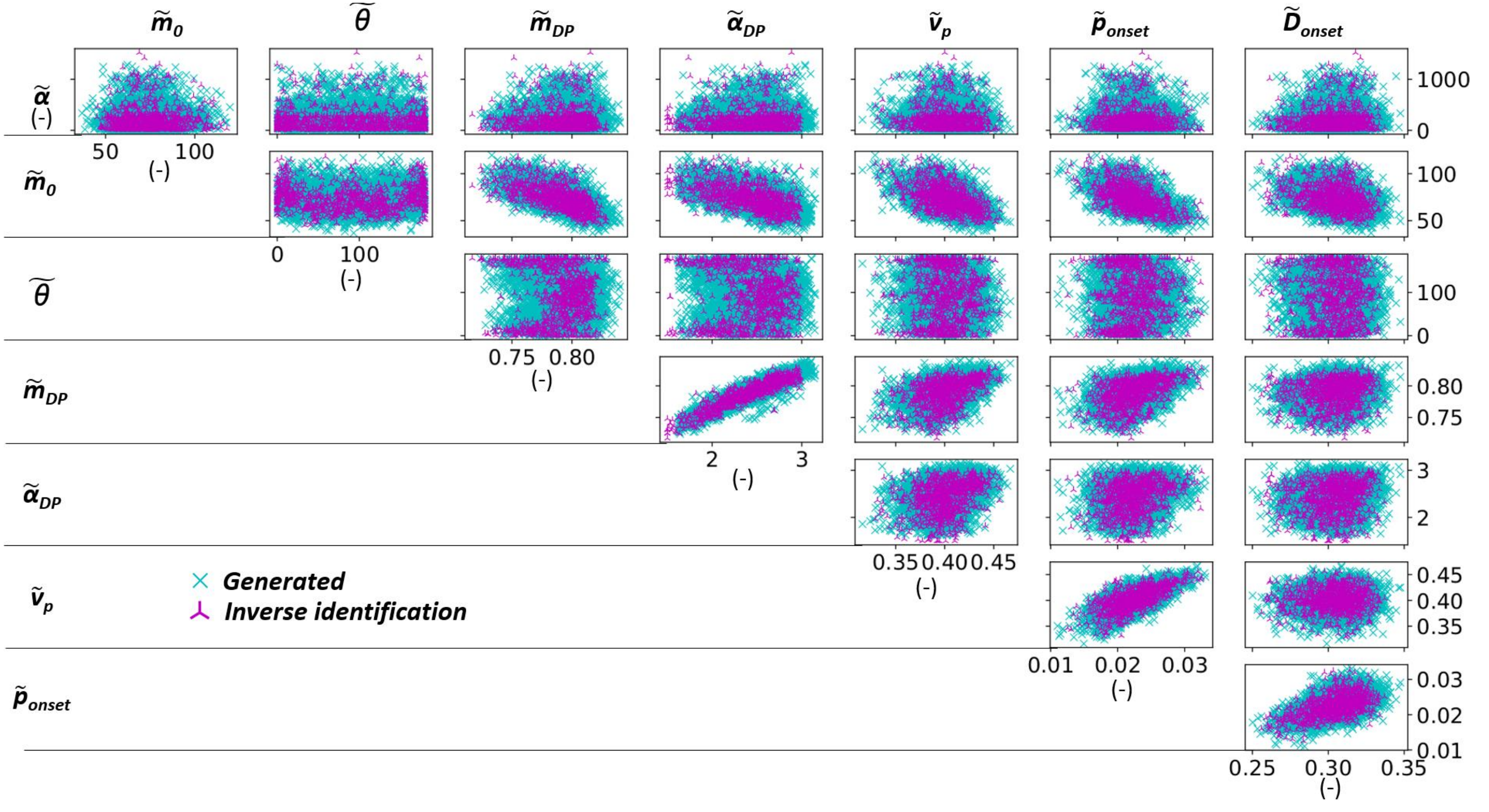

Stochastic MF-ROM

- Parameters are identified for 1050 SVE
- New data is generated using a Markov chain Monte Carlo (MCMC) process in order to obtain proper random fields

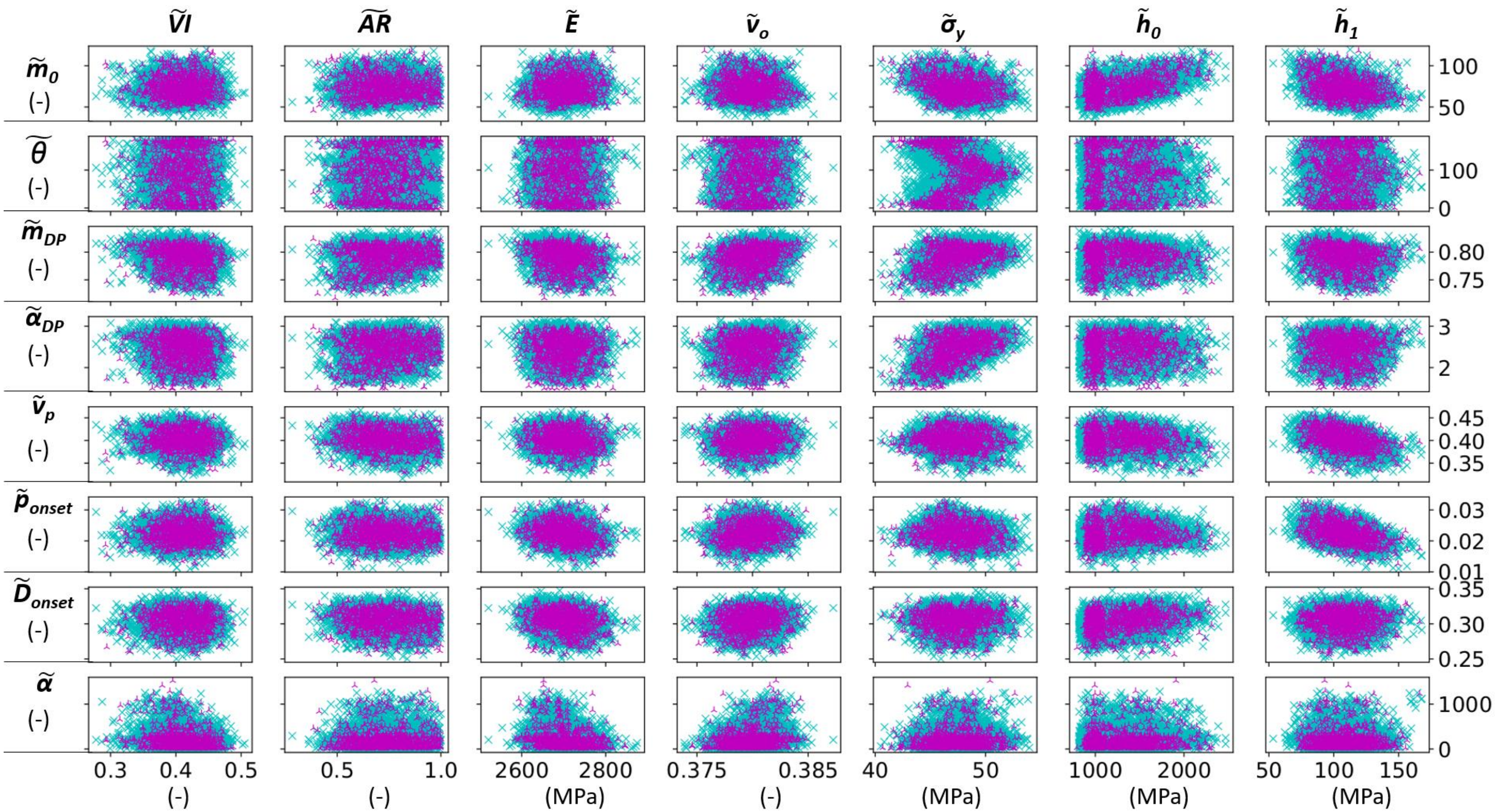

Stochastic MF-ROM

- The identified parameters yield good results for the wide range of SVE used

Uniaxial Tension

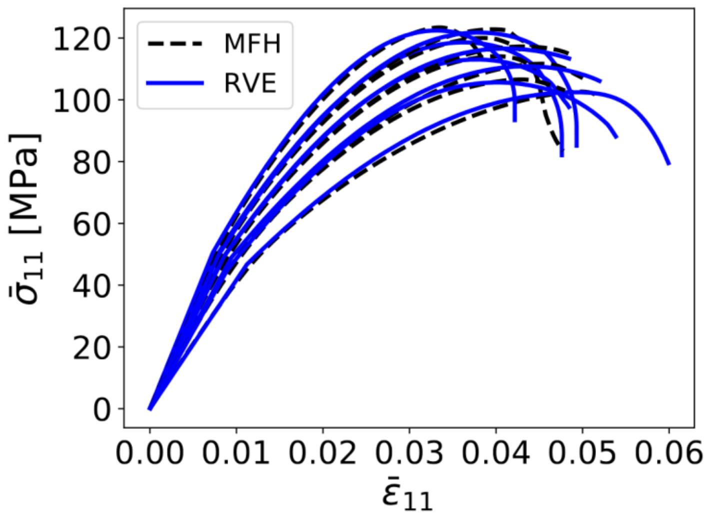

Uniaxial Compression

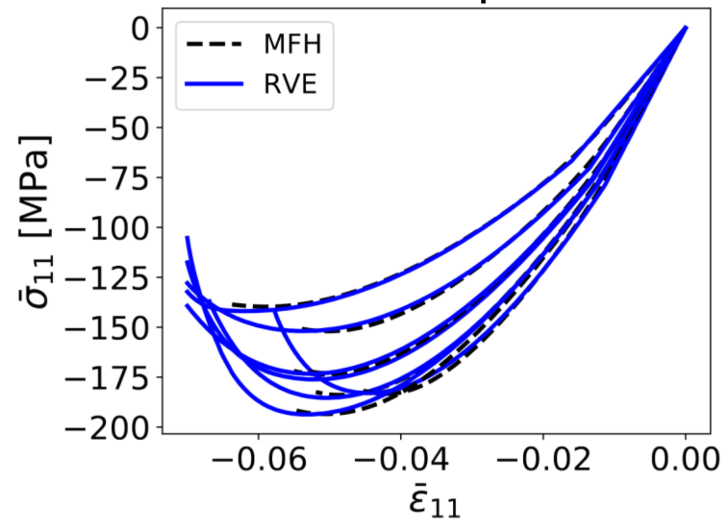

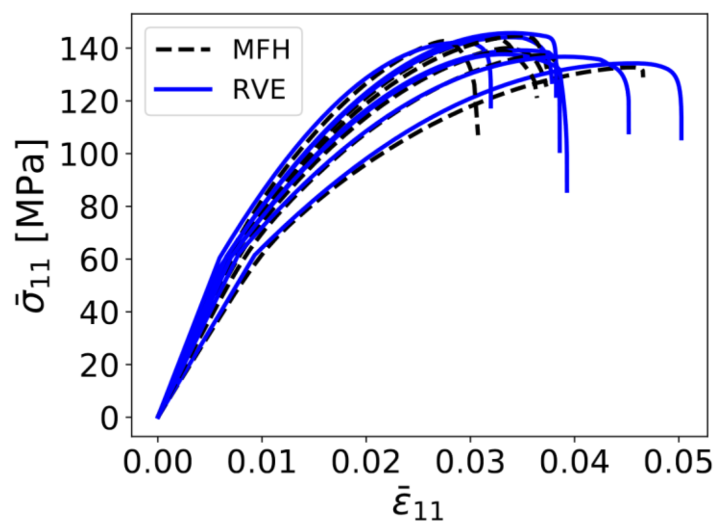

Biaxial

Stochastic MF-ROM Verification

- Tensile tests on 500 x 250 µm composite ply are performed using full-field and stochastic MFH simulations

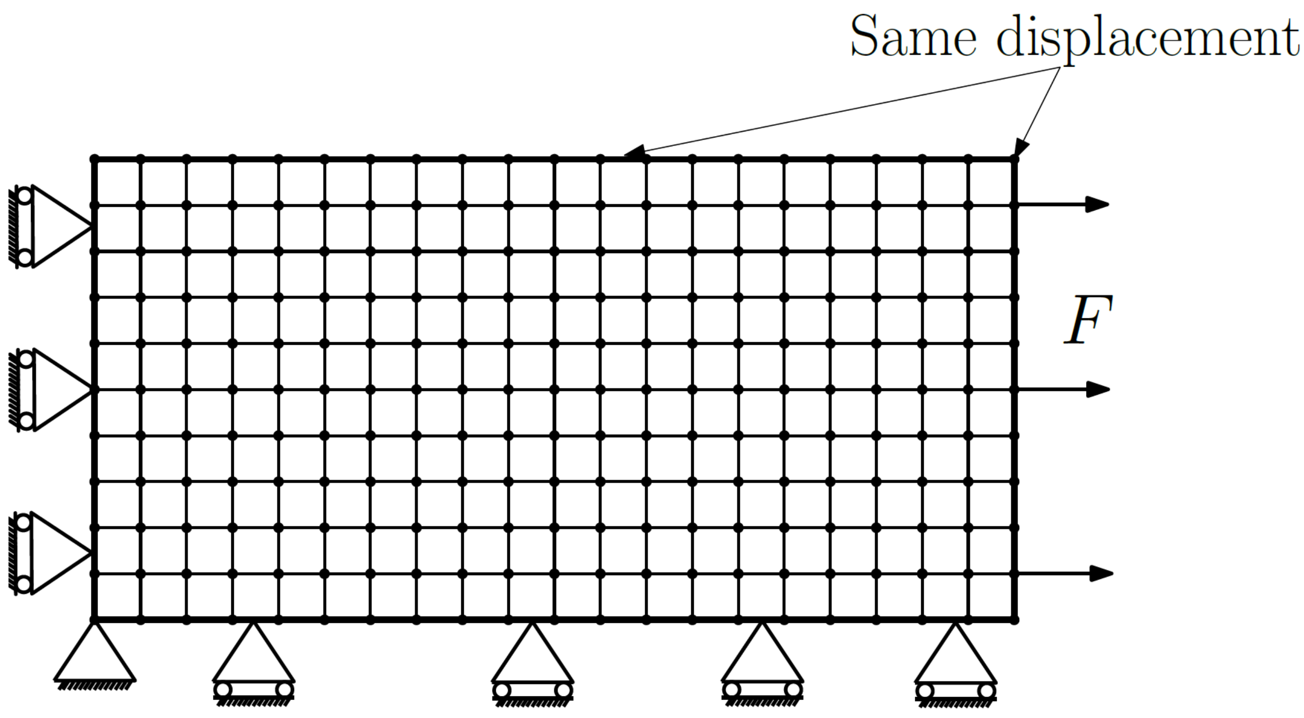

Stochastic MF-ROM Verification

- Tensile tests on 500 x 250 μm composite ply are performed using full-field and stochastic MFH simulations

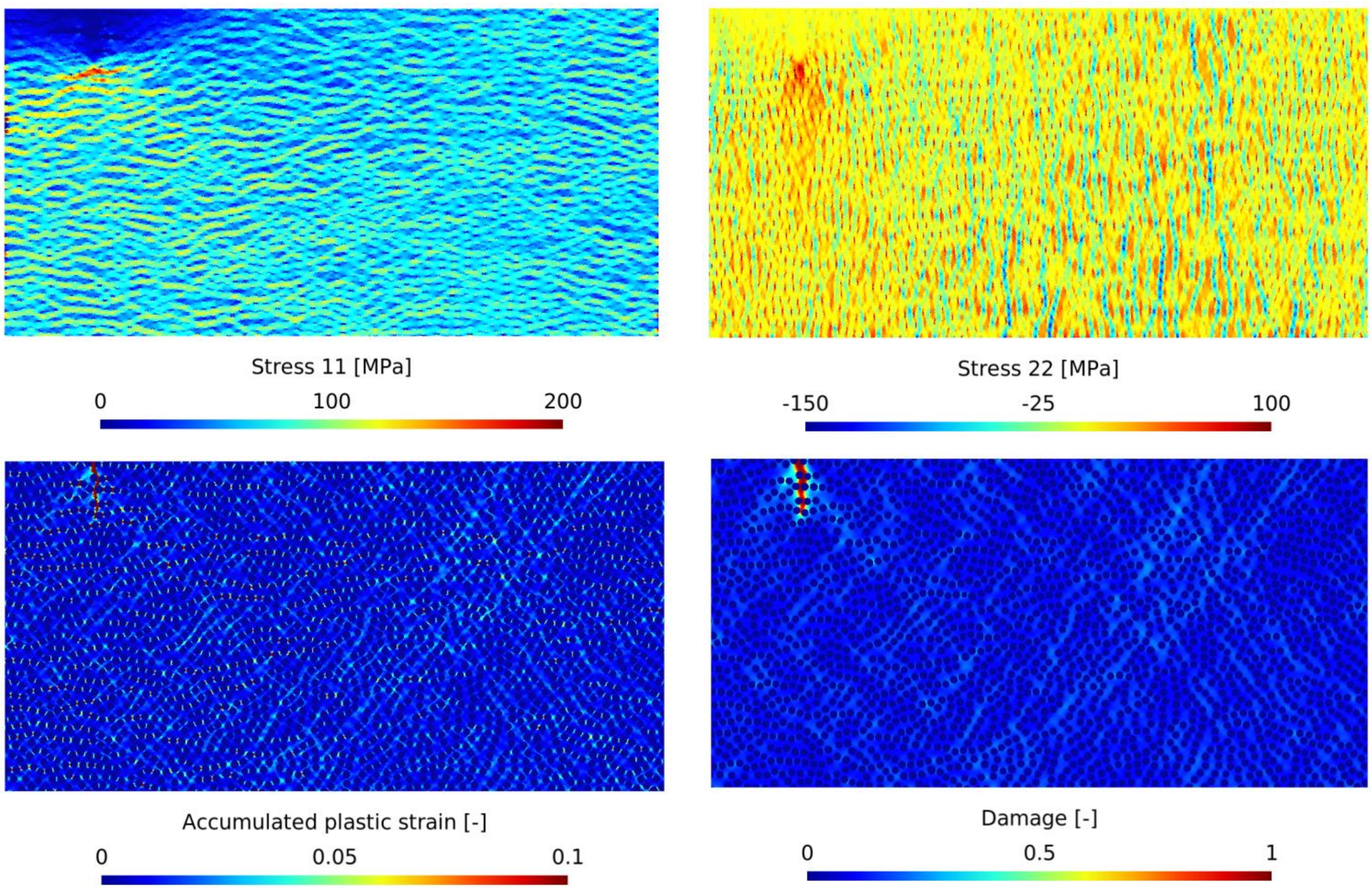

Stochastic MF-ROM Verification

- Tensile tests on 500 x 250 µm composite ply are performed using full-field and stochastic MFH simulations

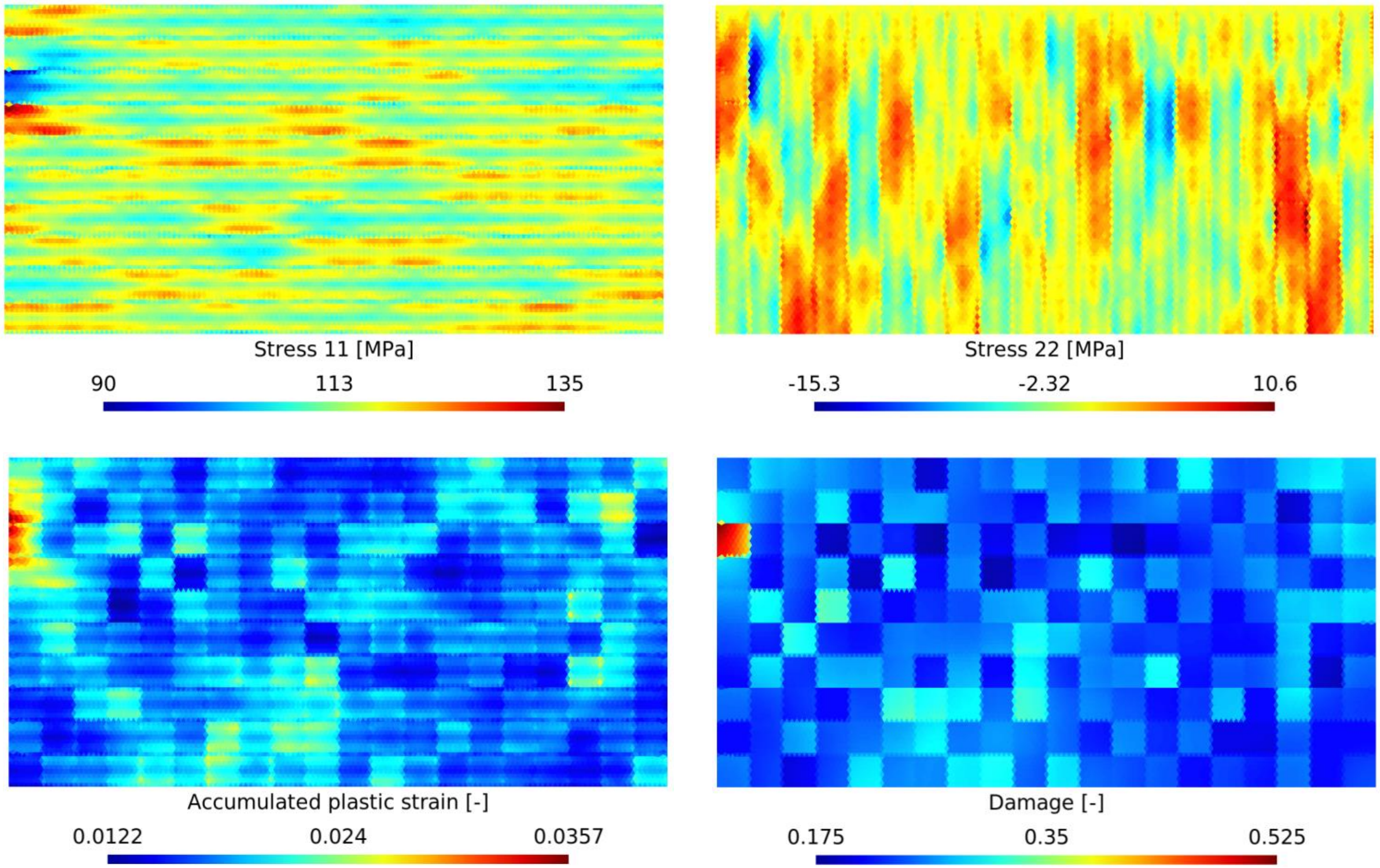

Stochastic MF-ROM Verification

- Tensile tests on 500 x 250 μm composite ply are performed using full-field and stochastic MFH simulations

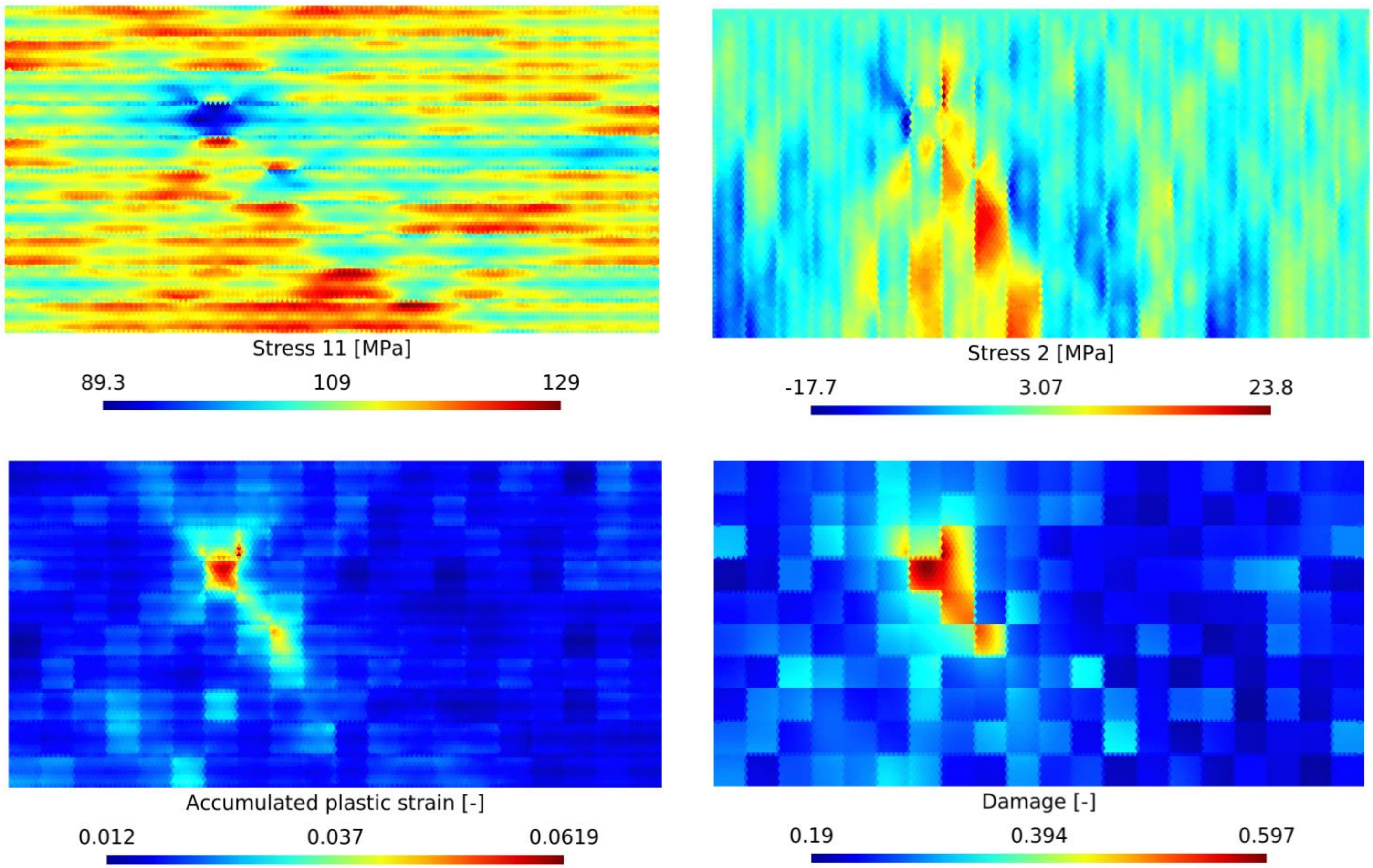

Stochastic MF-ROM Verification

- Tensile tests on 500 x 250 µm composite ply are performed using full-field and stochastic MFH simulations

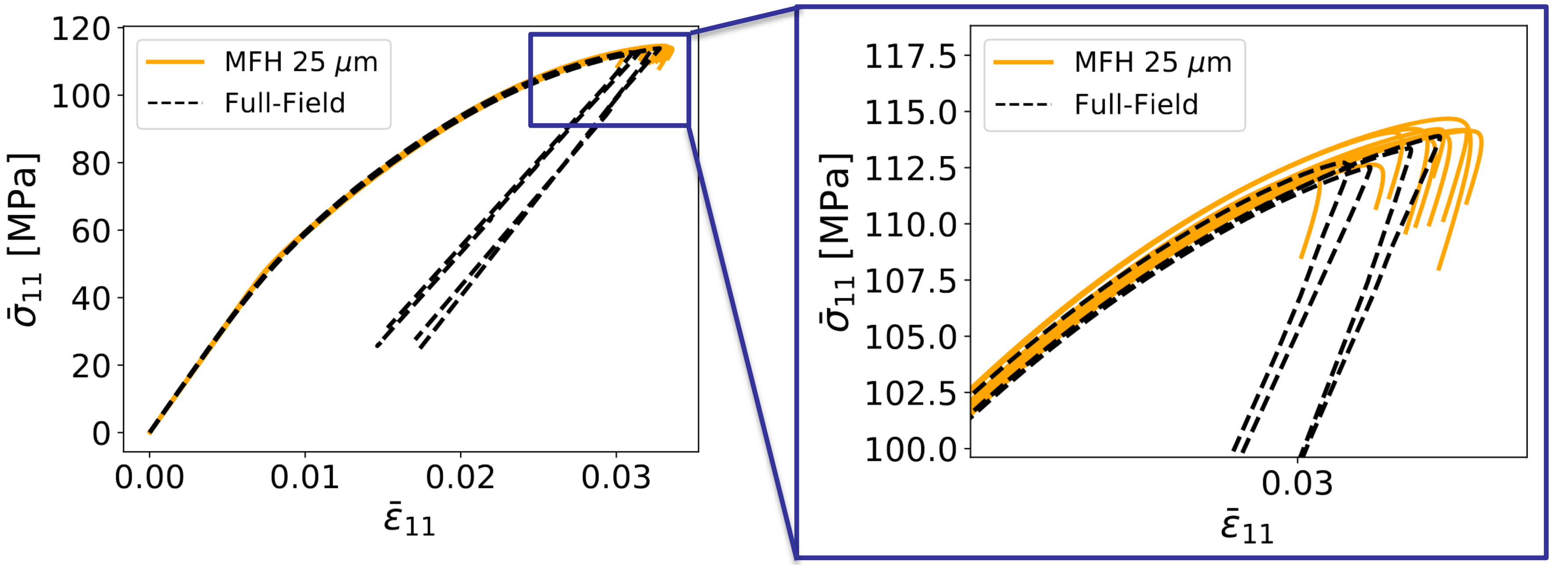

Conclusion and Future Work

- The MFH implementation of the pressure dependent plasticity model shows good agreement between the full-field simulations and the MFH simulations for all test cases

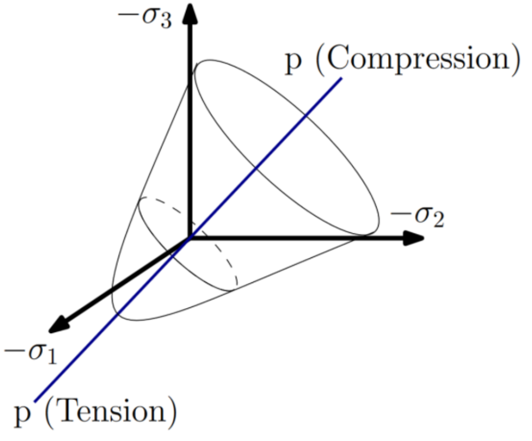

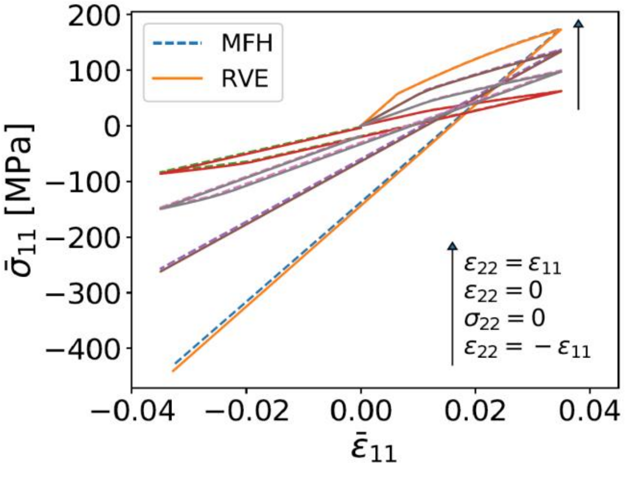

Conclusion and Future Work

- The MFH implementation of the pressure dependent plasticity model shows good agreement between the full-field simulations and the MFH simulations for all test cases

- The parameter identification process is robust and is capable of successfully represent a wide variety of SVE up to their total failure

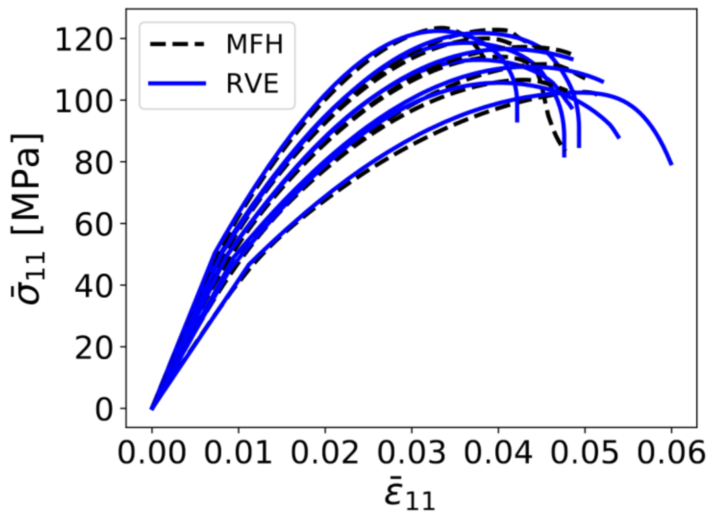

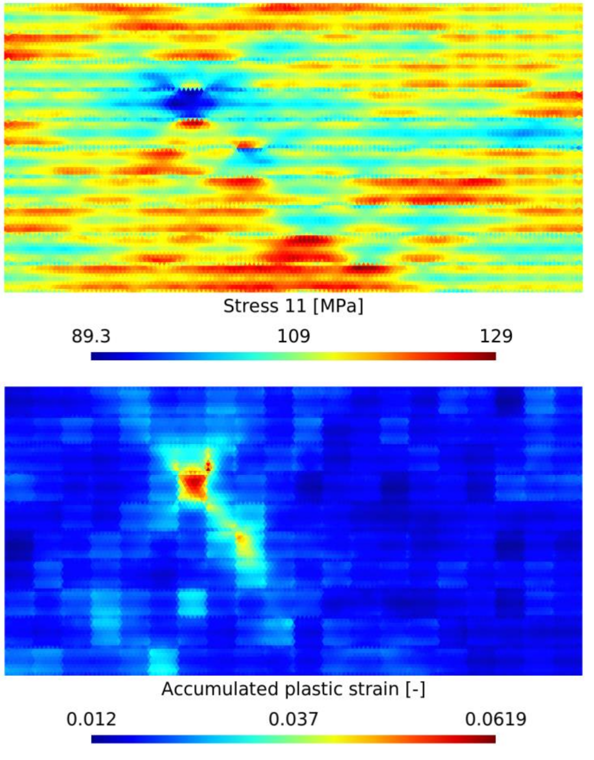

Conclusion and Future Work

- The MFH implementation of the pressure dependent plasticity model shows good agreement between the full-field simulations and the MFH simulations for all test cases
- The parameter identification process is robust and is capable of successfully represent a wide variety of SVE up to their total failure
- The build process of the stochastic MF-ROM offers high flexibility, allowing to further enrich it in future works with more complex hardening and damage evolution laws
- This MF-ROM could be used in the modelling of multiscale woven composites

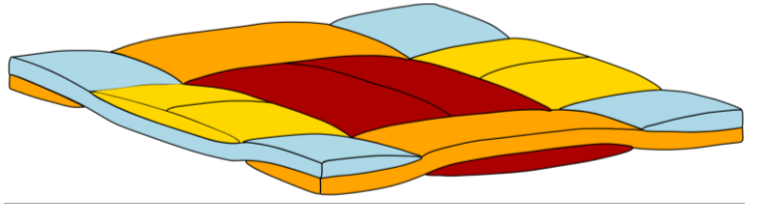

Special thanks to:

Wallonie
STOMMMAC project

fnrs
LA LIBERTÉ DE CHERCHER

References

- L. Wu, V.-D. Nguyen, L. Adam, L. Noels, An inverse micro-mechanical analysis toward the stochastic homogenization of nonlinear random composites, Comp. Meth. in App. Mech. and Engineering (ISSN: 0045-7825) 348, (2019) 97-138, https://doi.org/10.1016/j.cma.2019.01.016
- L. Wu, C.N. Chung, Z. Major, L. Adam, L. Noels, From SEM images to elastic responses: A stochastic multiscale analysis of UD fiber reinforced composites, Compos. Struct. (ISSN: 0263-8223) 189 (2018a) 206–227, http://dx.doi.org/10.1016/j.compstruct.2018.01.051
- L. Wu, C. Nghia Chung, Z. Major, L. Adam, L. Noels, A micro-mechanics-based inverse study for stochastic order reduction of elastic UD-fiber reinforced composites analyzes, Internat. J. Numer. Methods Engrg. (ISSN: 0263-8223) 115 (2018b) 1430–1456, http://dx.doi.org/10.1016/
- T. Mori, K. Tanaka, Average stress in matrix and average elastic energy of materials with misfitting inclusions, Acta Metall. 21 (5) (1973) 571–574
- L. Wu, L. Noels, L. Adam, I. Doghri, A combined incremental–secant mean–field homogenization scheme with per–phase residual strains for elasto–plastic composites, Int. J. Plast. 51 (2013a) 80–102, http://dx.doi.org/10.1016/j.ijplas.2013.06.006
- L. Wu, L. Noels, L. Adam, I. Doghri, An implicit-gradient-enhanced incremental-secant mean-field homogenization scheme for elasto-plastic composites with damage, Int. J. Solids Struct. (ISSN: 0020-7683) 50 (24) (2013b) 3843–3860, http://dx.doi.org/10.1016/j.ijsolstr.2013.07.022.
- L. Wu, L. Adam, I. Doghri, L. Noels, An incremental-secant mean-field homogenization method with second statistical moments for elasto-visco-plastic composite materials, Mech. Mater. (ISSN: 0167-6636) 114 (2017) 180–200, http://dx.doi.org/10.1016/j.mechmat.2017.08.006.
- V.-D.Nguyen F.Lani T.Pardoen X.P.Morelle L.Noels, A large strain hyperelastic viscoelastic-viscoplastic-damage constitutive model based on a multi-mechanism non-local damage continuum for amorphous glassy polymers. Int. Journal of Sol. and Struct., (ISSN: 0020-7683) 96 (2016) 192-216, https://doi.org/10.1016/j.ijsolstr.2016.06.008
- V.-D. Nguyen, L. Wu, L. Noels, A micro-mechanical model of reinforced polymer failure with length scale effects and predictive capabilities. Validation on carbon fiber reinforced high-crosslinked RTM6 epoxy resin , Mech. Mater. (ISSN: 0167-6636) 133 (2019) 193-213, https://dx.doi.org/10.1016/j.mechmat.2019.02.017


Q&A

Enhanced Drucker-Prager: Incremental Secant Implementation

- The plastic correction reads:

$$\Delta p = k\Gamma\sqrt{\boldsymbol{N}:\boldsymbol{N}} = k\Gamma\sqrt{6\left((\hat{\boldsymbol{\sigma}}_{n+1} - \hat{\boldsymbol{\sigma}}_n^{res})^{eq}\right)^2 + \frac{4}{3}\beta^2\left(\hat{\boldsymbol{\phi}}_{n+1} - \hat{\boldsymbol{\phi}}_n^{res}\right)^2}$$

$$(\hat{\boldsymbol{\sigma}}_{n+1} - \hat{\boldsymbol{\sigma}}_n^{res})^{dev} = (\hat{\boldsymbol{\sigma}}_{n+1}^{tr} - \hat{\boldsymbol{\sigma}}_n^{res})^{dev} - 2\mu^{el}\Gamma\left(3(\hat{\boldsymbol{\sigma}}_{n+1} - \hat{\boldsymbol{\sigma}}_n^{res})^{dev}\right) = \frac{(\hat{\boldsymbol{\sigma}}_{n+1}^{tr} - \hat{\boldsymbol{\sigma}}_n^{res})^{dev}}{1 + 6\mu^{el}\Gamma}$$

$$(\hat{\boldsymbol{\sigma}}_{n+1} - \hat{\boldsymbol{\sigma}}_n^{res})^{vol} = (\hat{\boldsymbol{\sigma}}_{n+1}^{tr} - \hat{\boldsymbol{\sigma}}_n^{res})^{vol} - 3\kappa^{el}\Gamma\left(\frac{2\beta}{3}(\hat{\boldsymbol{\sigma}}_{n+1} - \hat{\boldsymbol{\sigma}}_n^{res})^{vol}\right) = \frac{(\hat{\boldsymbol{\sigma}}_{n+1}^{tr} - \hat{\boldsymbol{\sigma}}_n^{res})^{vol}}{(1 + 2\kappa^{el}\Gamma\beta)}$$

$$\hat{\boldsymbol{\sigma}}^{vol} = \hat{\phi}\boldsymbol{I} \qquad \nu_p = \frac{9 - 2\beta}{18 + 2\beta}$$

- It is then possible to define C^{sr}, which writes:

$$\boldsymbol{C}^{Sr} = \boldsymbol{C}^{el} - \frac{6\mu^{el}\Gamma}{1 + 6\mu^{el}\Gamma}(\boldsymbol{I}^{dev}:\boldsymbol{C}^{el}) - \frac{2\beta\kappa^{el}\Gamma}{1 + 2\kappa^{el}\Gamma\beta}(\boldsymbol{I}^{vol}:\boldsymbol{C}^{el})$$

- C^{sr} is found to be isotropic, being possible to identify μ_s^r and κ_s^r as:

$$\kappa_s^r = \kappa^{el} - \frac{2\beta\kappa^{el^2}\Gamma}{1 + 2\kappa^{el}\Gamma\beta} \qquad \mu_s^r = \mu^{el} - \frac{6\mu^{el^2}\Gamma}{1 + 6\mu^{el}\Gamma}$$

Enhanced Drucker-Prager: Incremental Secant Implementation

- It is then possible to compute the damage-enhanced residual-incremental secant operator and the final stress as:

$$\boldsymbol{C}^{SDr} = (1 - D_{n+1})\boldsymbol{C}^{Sr}$$

$$\boldsymbol{\sigma}_{n+1} = (1 - D_{n+1})\hat{\boldsymbol{\sigma}}_n^{res} + \boldsymbol{C}^{SDr} : \Delta\boldsymbol{\varepsilon}_{n+1}^r$$

- Consequently, the damaged bulk and shear moduli read:

$$\kappa_S^{Dr} = (1 - D_{n+1})\left(\kappa^{el} - \frac{2\beta {\kappa^{el}}^2 \Gamma}{1 + 2\beta\kappa^{el}\Gamma}\right)$$

$$\mu_S^{Dr} = (1 - D_{n+1})\left(\mu^{el} - \frac{6 {\mu^{el}}^2 \Gamma}{1 + 6\mu^{el}\Gamma}\right)$$

- The MFH scheme was tested using Uni-Directional (UD) composite and spherical inclusions-reinforced matrix using periodic BC
  - 150x150 µm UD RVE 18, 28 and 40% fiber volume fraction
  - 100x100x100 µm spherical inclusions-reinforced RVE 20% fiber volume fraction

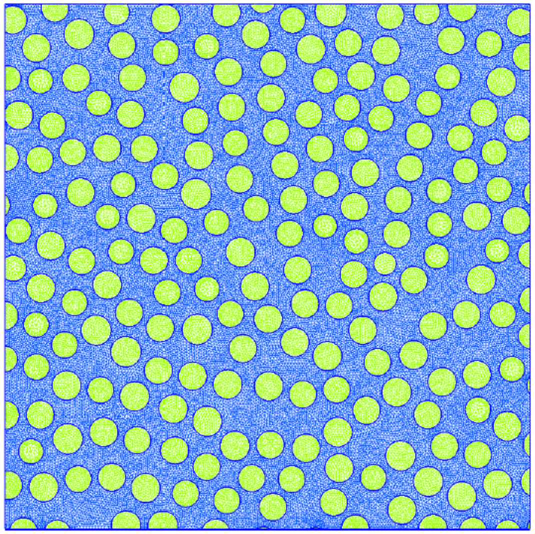

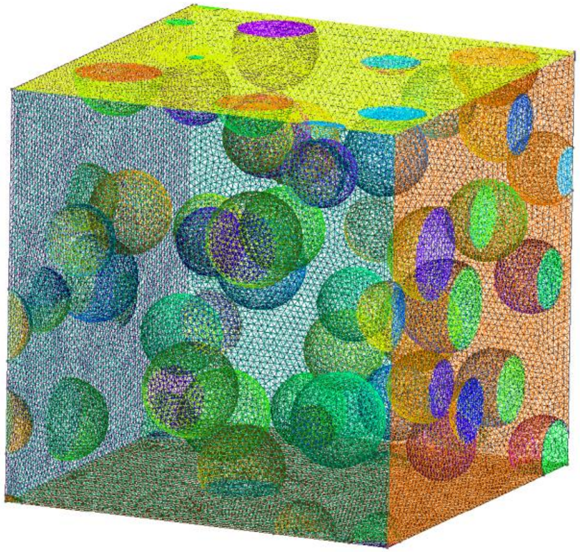

MFH verification : No damage

- Pressure Dependency:

Tension → Compression

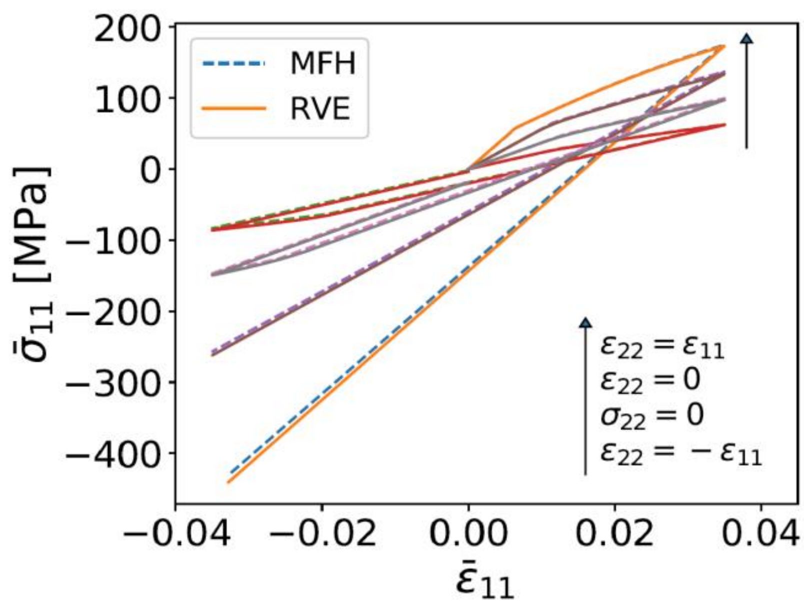

Compression→ Tension

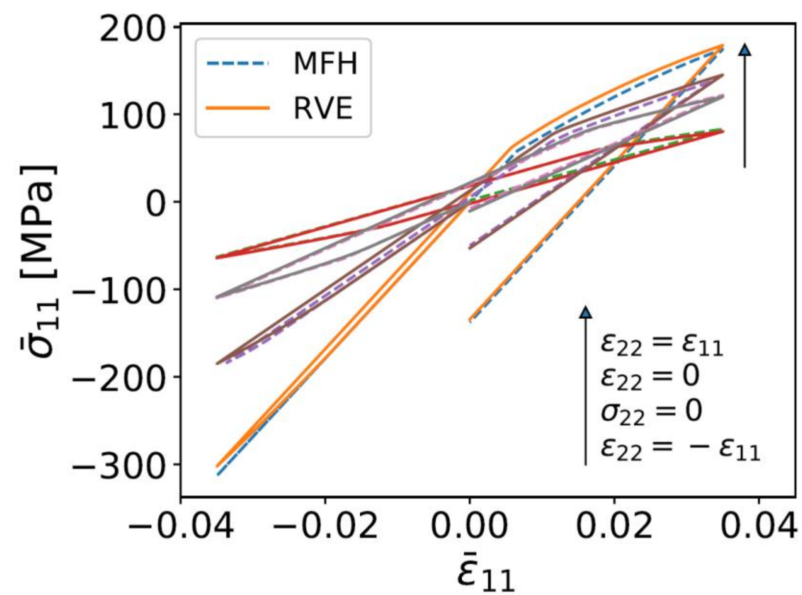

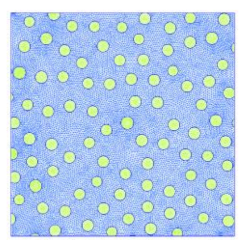

18%
Volume
Fraction

- Volume Fraction Dependency: Uniaxial Example

Phases

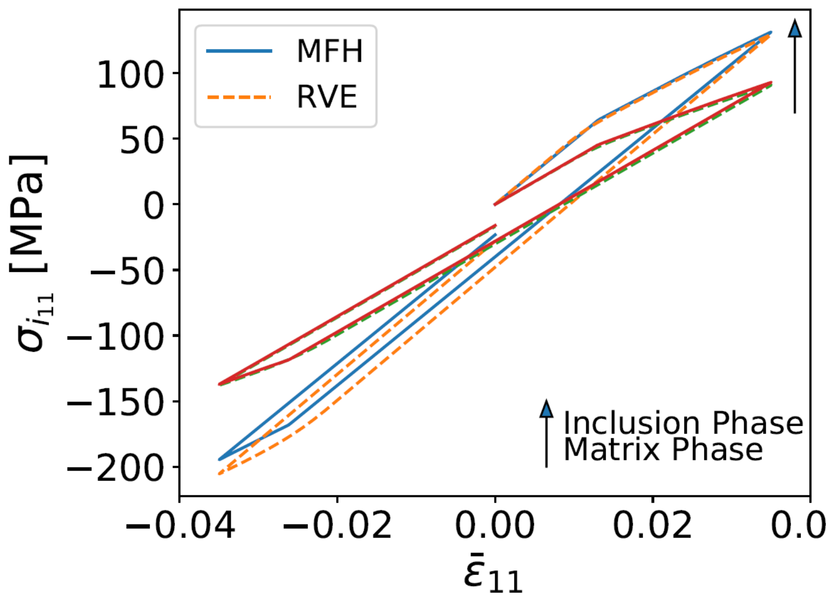

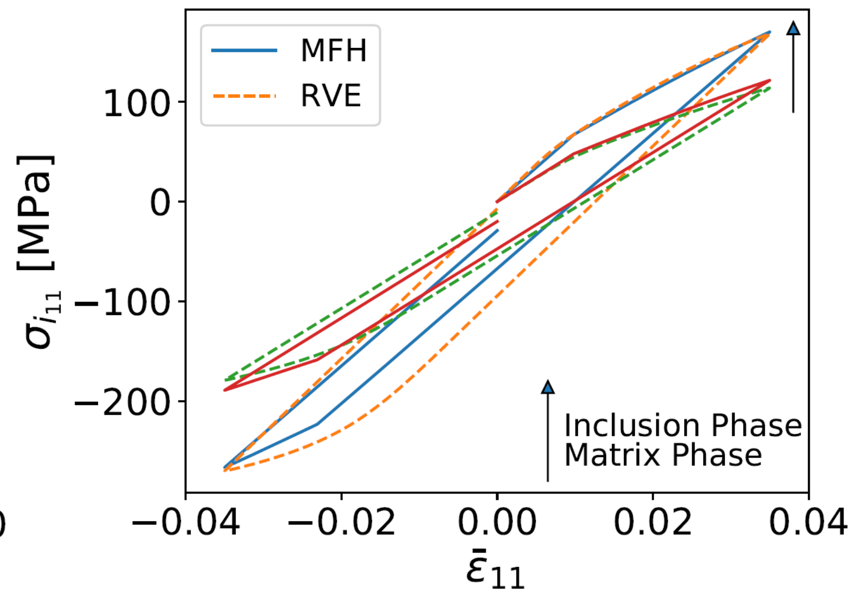

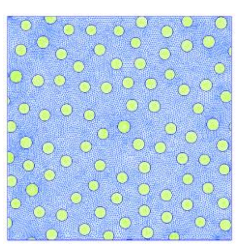

18% Volume Fraction

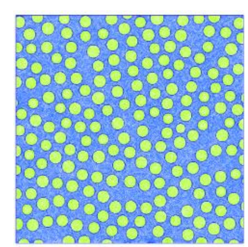

40% Volume Fraction

MFH verification : No damage

- Non-Proportional Loading

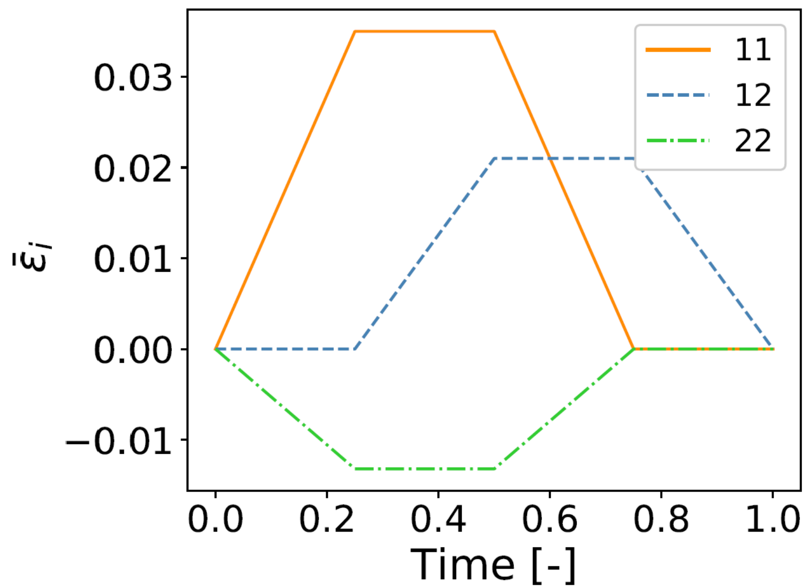

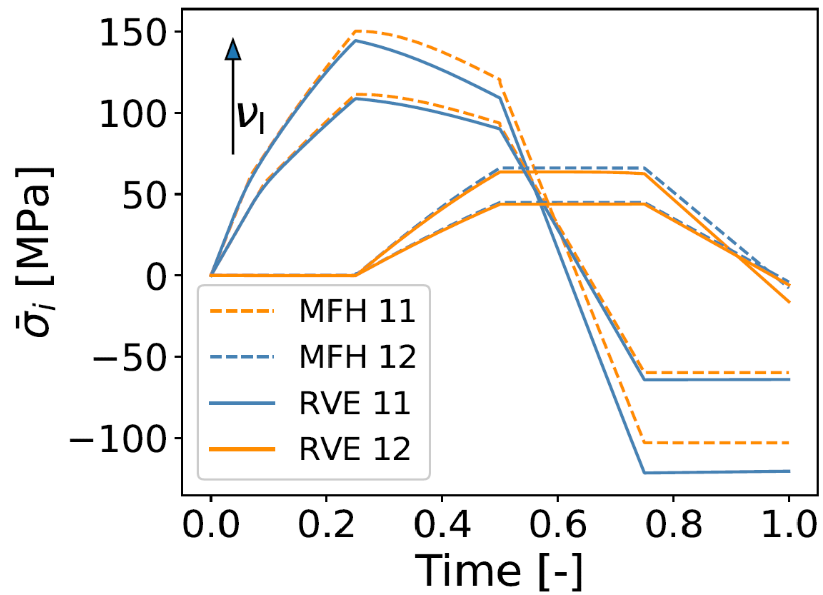

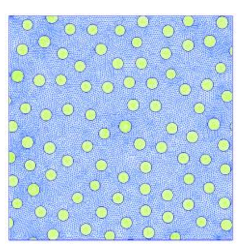

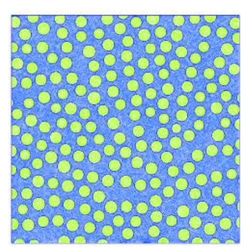

18% and 40% Volume Fractions

- Non-Proportional Loading

Phases

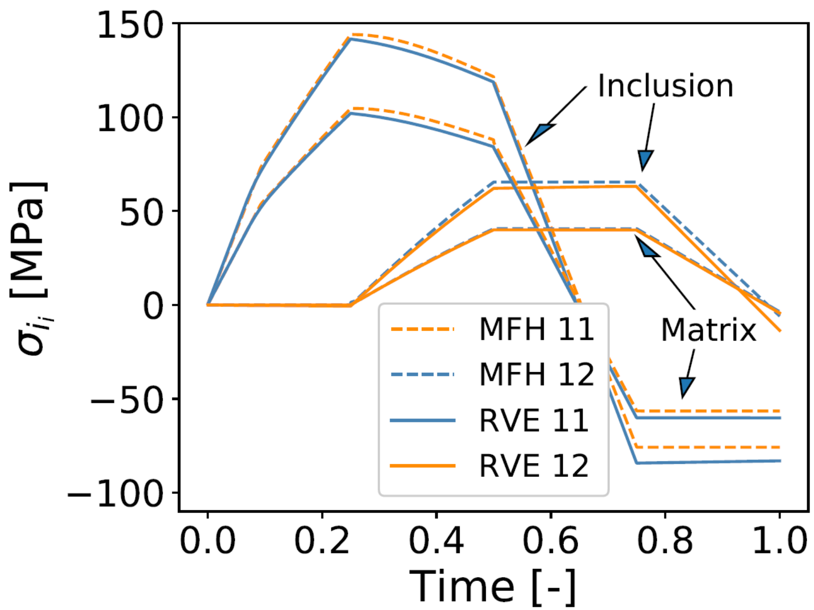

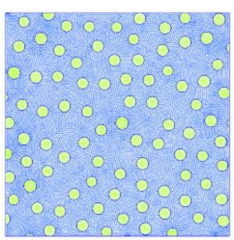

18%
Volume
Fraction

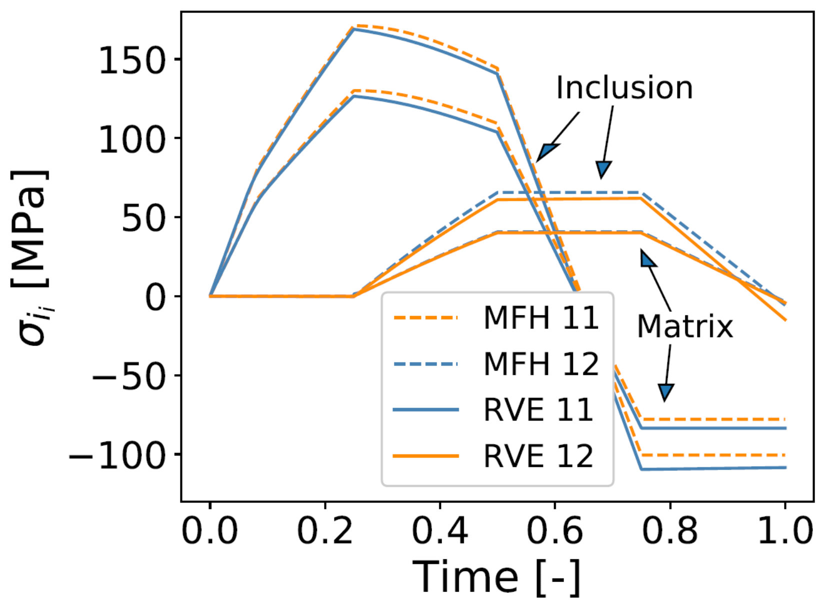

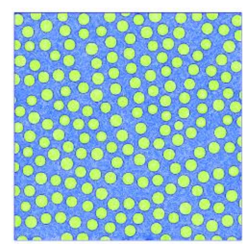

40%
Volume
Fraction

- 40% Composite

Composite

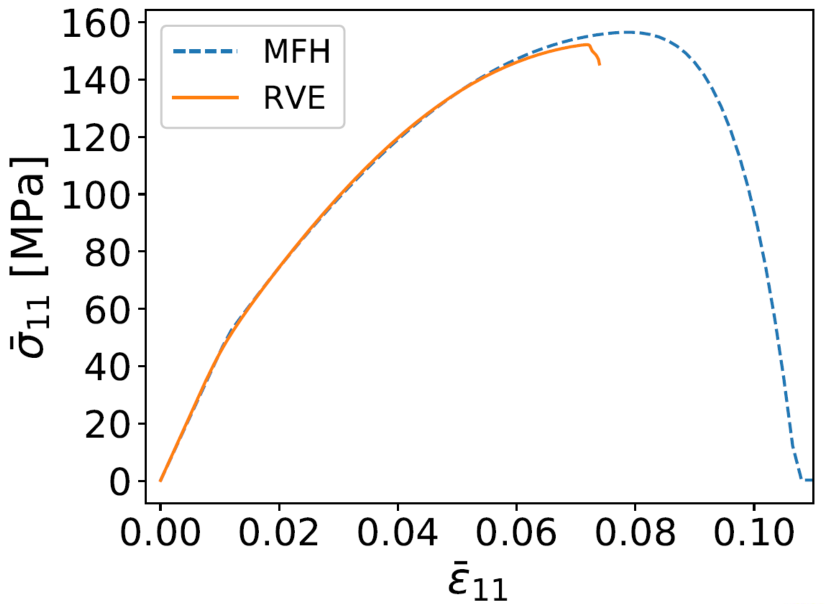

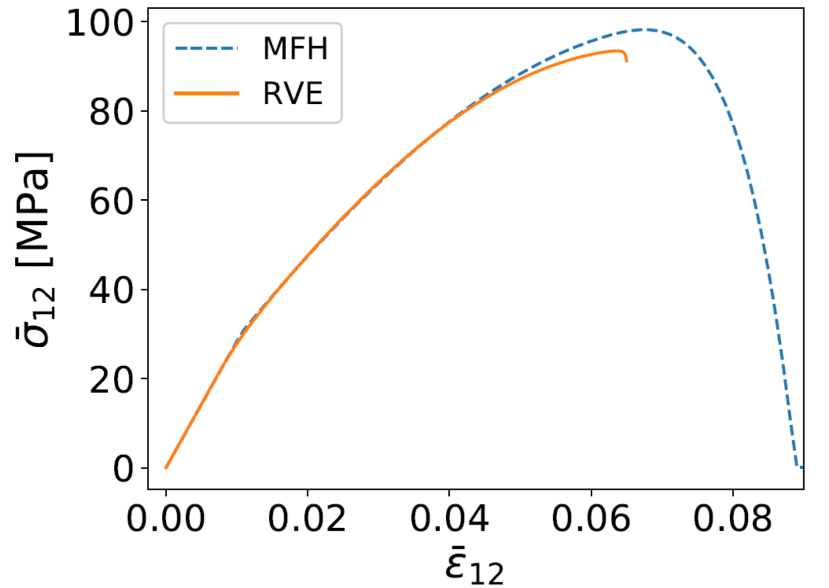

Uniaxial Tension

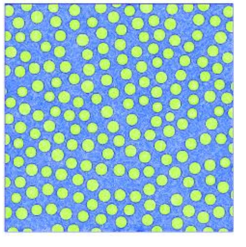

Shear Tension

- 40% Composite

Phases

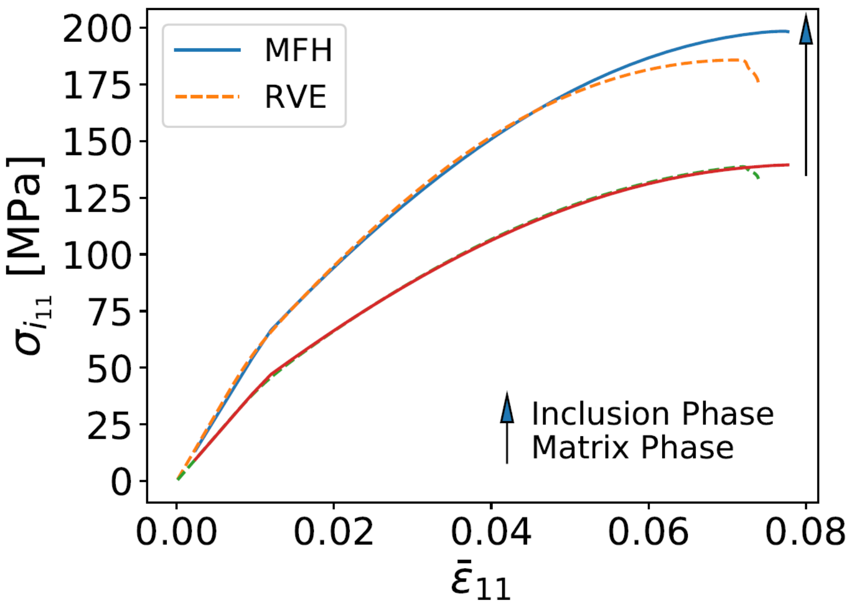

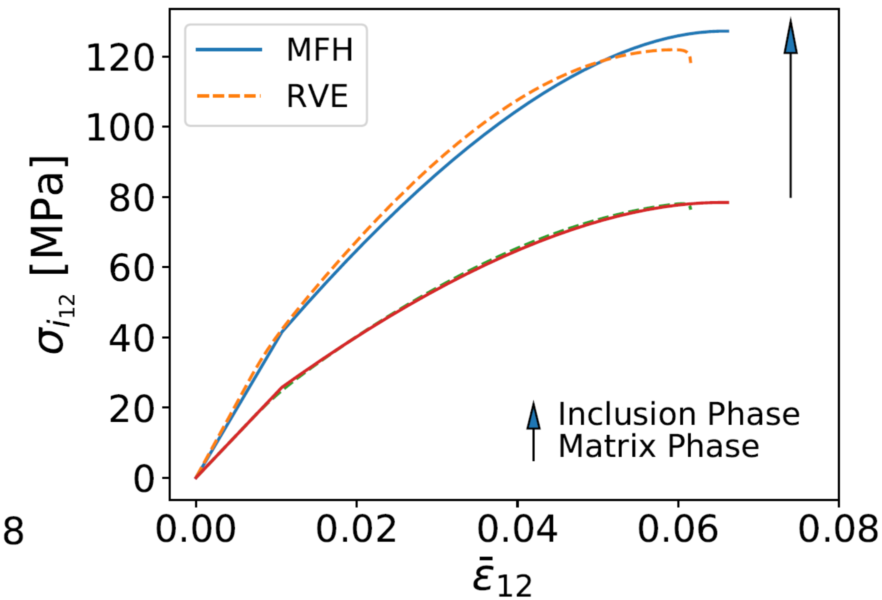

Uniaxial Tension

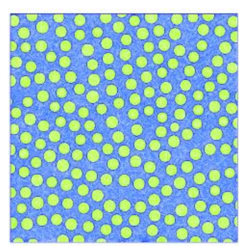

Shear Tension

MFH verification: 3D

- Spherical inclusions-reinforced matrix
- 100x100x100 µm RVE 20% fiber volume fraction
- Periodic boundary conditions under different loadings including uniaxial, triaxial, non-proportional and shear

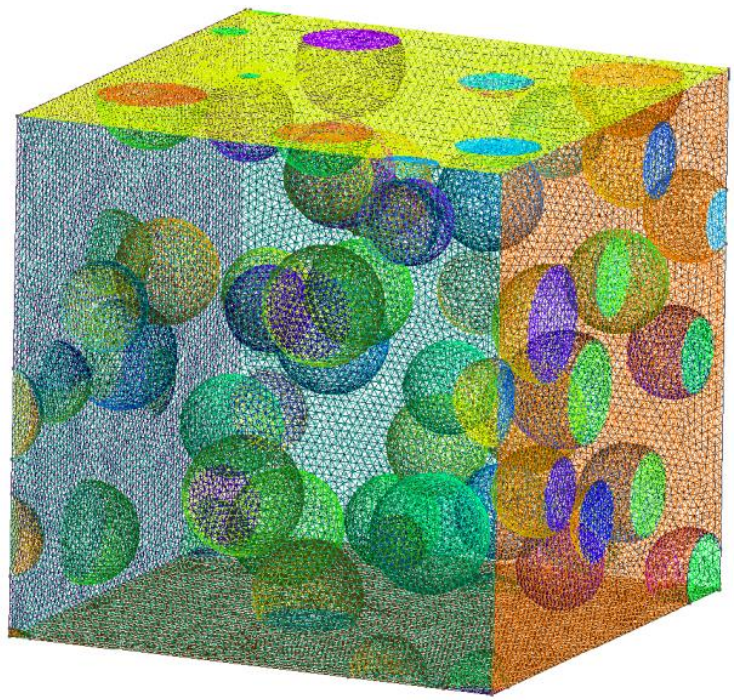

- Shear Loading

Composite

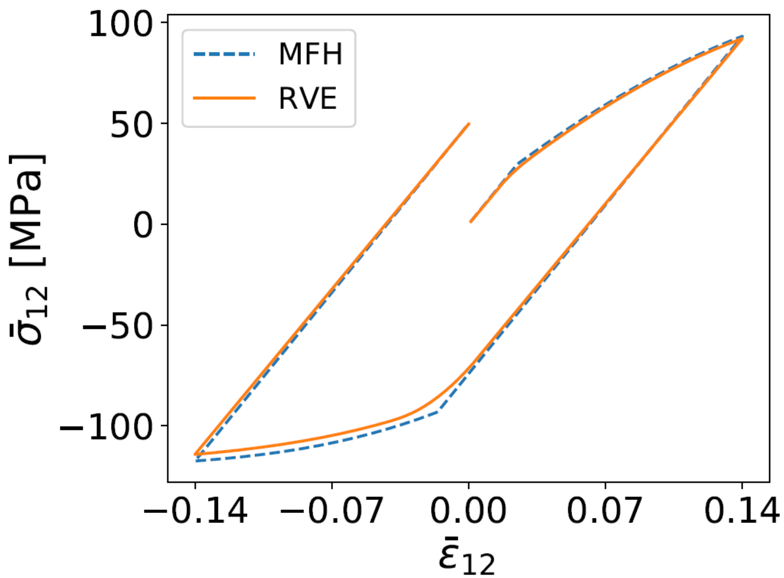

Phases

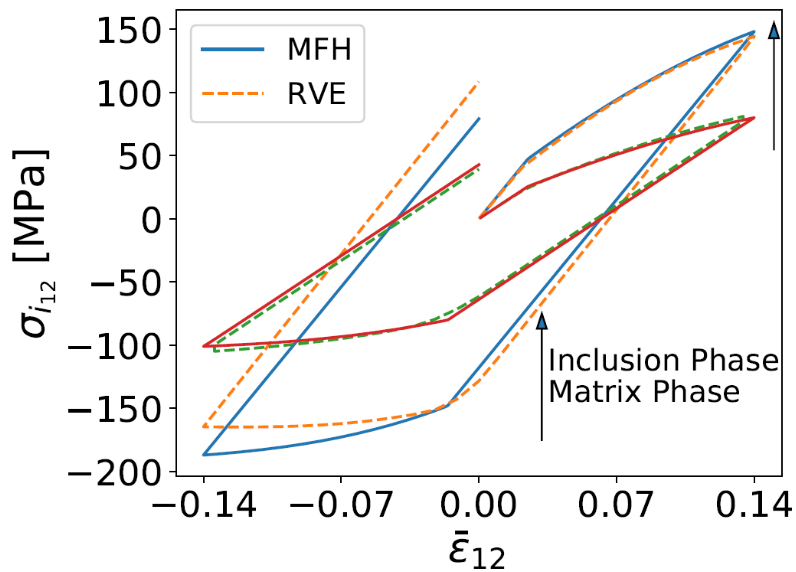

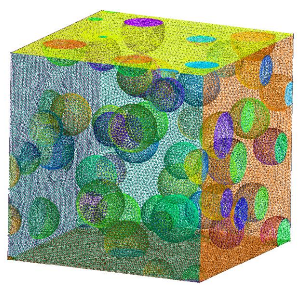

20% Volume Fraction

MFH verification: Experimental Compression Test

- Experimental test carried out in J. Chevalier et al. on UD composite
- 10x10x10 mm cubic sample with 40% fiber volume fraction
- Transverse compression test at a loading rate of $1^{-4}s^{-1}$

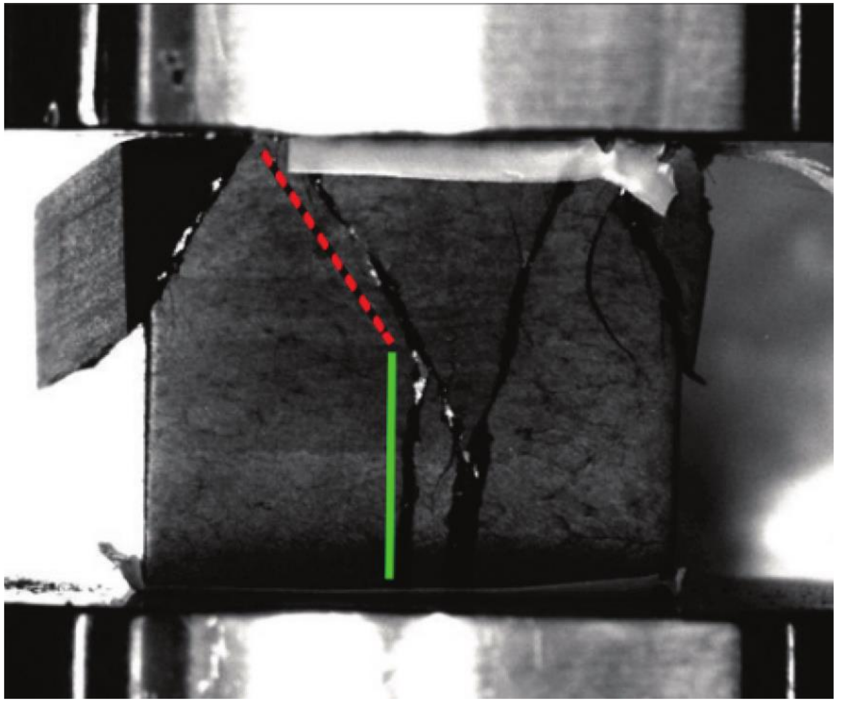

Chevalier J, Camanho P, Pardoen T. Multi-scale characterization and modelling of the transverse compression response of unidirectional carbon fiber reinforced epoxy. *Comp. Struct.* 2019

MFH verification: Experimental Compression Test

- Experimental test carried out in J. Chevalier et al. on UD composite
- 10x10x10 mm cubic sample with 40% fiber volume fraction
- Transverse compression test at a loading rate of $1^{-4}s^{-1}$

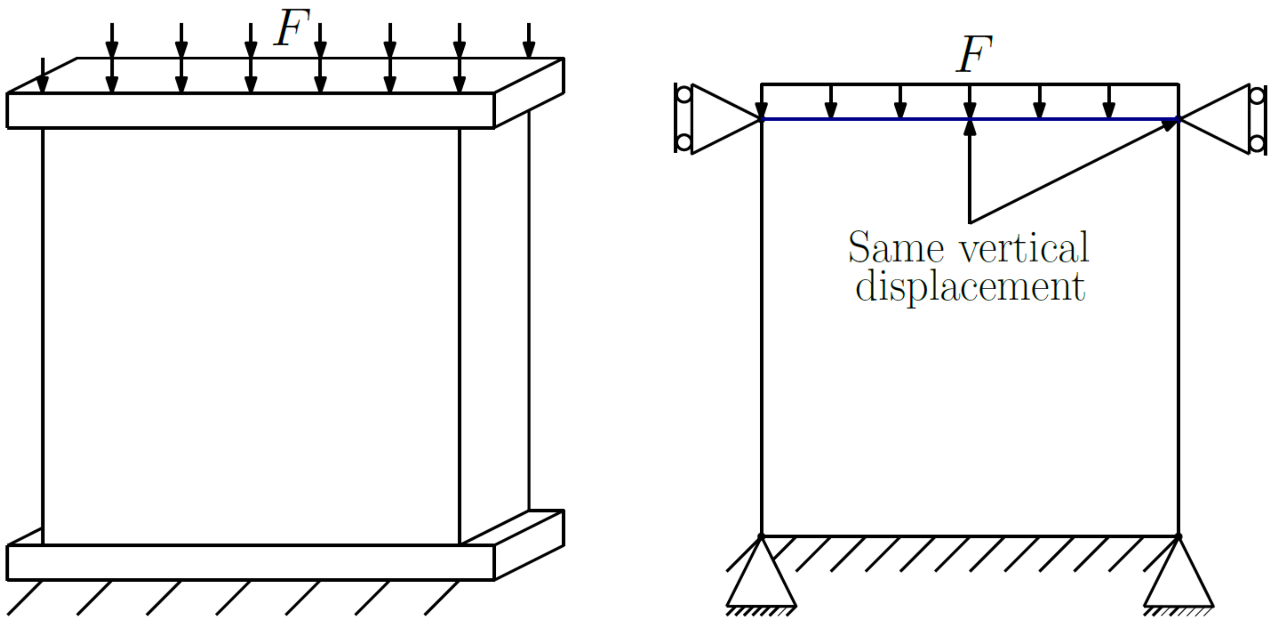

Chevalier J, Camanho P, Pardoen T. Multi-scale characterization and modelling of the transverse compression response of unidirectional carbon fiber reinforced epoxy. *Comp. Struct.* 2019

MFH verification: Experimental Compression Test

- Experimental test carried out in J. Chevalier et al. on UD composite
- 10x10x10 mm cubic sample with 40% fiber volume fraction
- Transverse compression test at a loading rate of $1^{-4}s^{-1}$

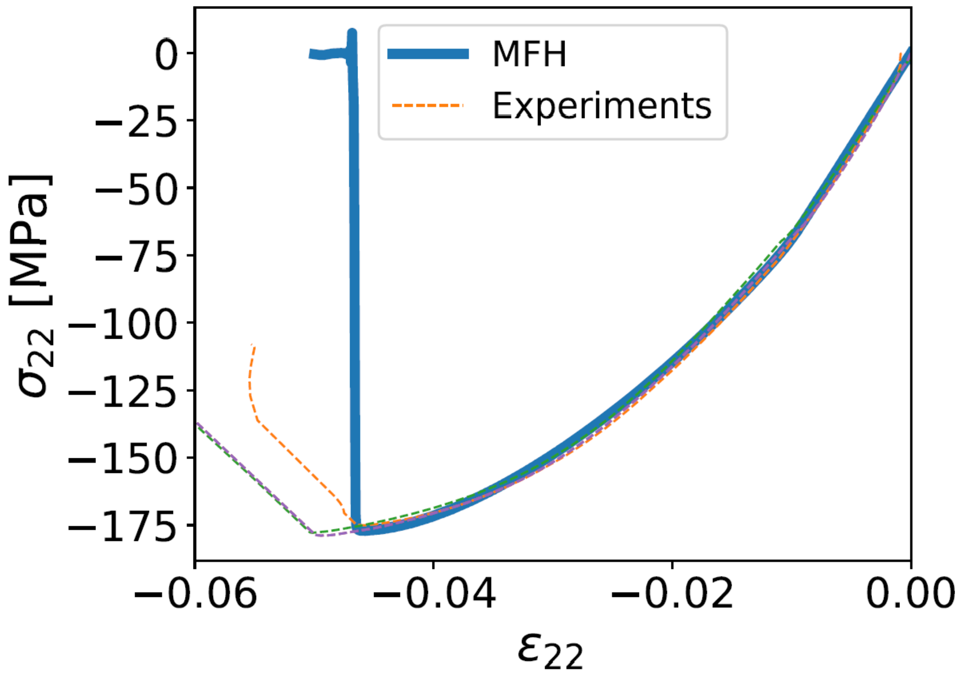

Chevalier J, Camanho P, Pardoen T. Multi-scale characterization and modelling of the transverse compression response of unidirectional carbon fiber reinforced epoxy. *Comp. Struct.* 2019

MFH verification: Experimental Compression Test

- Experimental test carried out in J. Chevalier et al. on UD composite
- 10x10x10 mm cubic sample with 40% fiber volume fraction
- Transverse compression test at a loading rate of $1^{-4}s^{-1}$

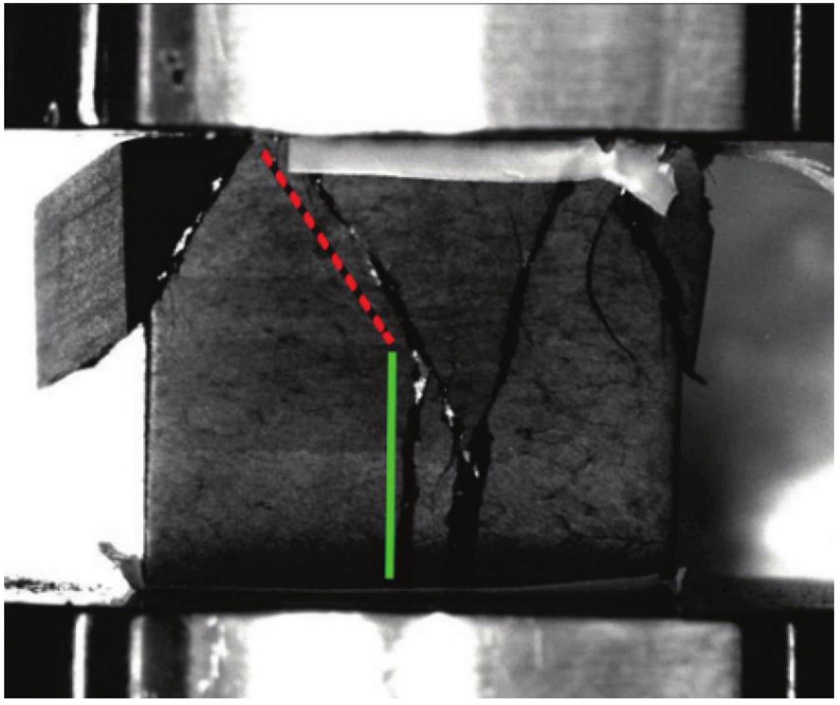

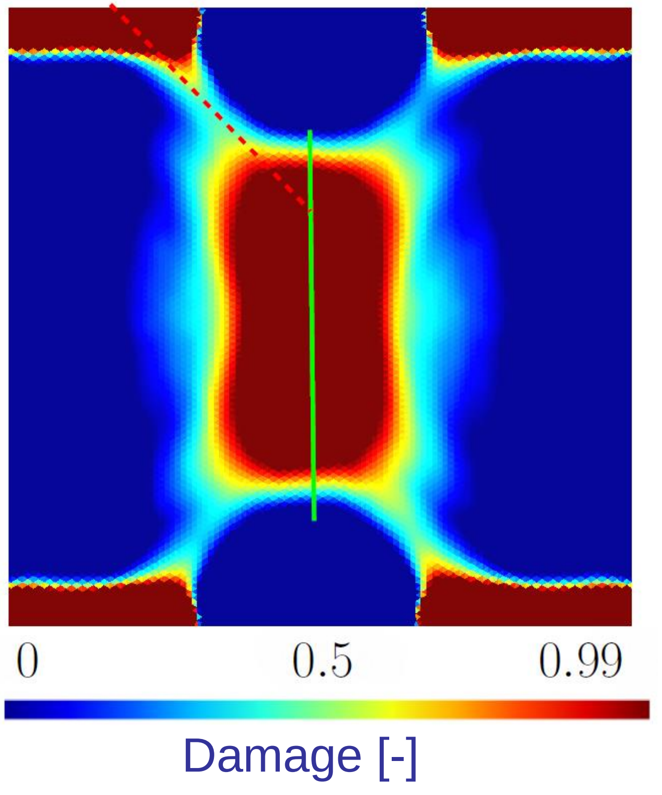

Chevalier J, Camanho P, Pardoen T. Multi-scale characterization and modelling of the transverse compression response of unidirectional carbon fiber reinforced epoxy. *Comp. Struct.* 2019

- Parameter identification of the two-part function damage model ($\tilde{p}_{onset}, \tilde{D}_{onset}, \tilde{\alpha}_{dam}, \ \tilde{\beta}_{dam}$):
  - Linear increase of damage up to the softening onset point
    - Rate of the damage evolution depends on the damage and the accumulated plastic strain at onset point → $\tilde{p}_{onset}$, and $\tilde{D}_{onset}$ obtained directly from the identified values at the softening onset

$$\dot{\tilde{D}}_0 = \frac{\tilde{D}_{Onset}}{\tilde{p}_{Onset}} \Delta \tilde{p}_0$$

  - After the softening onset, the parameters are identified to recover the SVE energy release (G_c), as it becomes the only objective value
  - $\min_{\tilde{f}_{Dam}} \left\{ \left| \Delta G_{c_{MFH}}(\tilde{f}_{Dam}) \right| \right\}$ where $\Delta G_{c_{MFH}}(\tilde{f}_{Dam}) = G_{c_{MFH}}(\tilde{f}_{Dam}) - G_{c_{SVE}}$
  - At each minimization step, an MFH simulation is performed in order to obtain this value

Damage-Enhanced Elasto-Plastic Identification

- In order to recover the equivalent MFH SVE G_c
  - L >> l ; W << l to obtain non-dimensional G_c

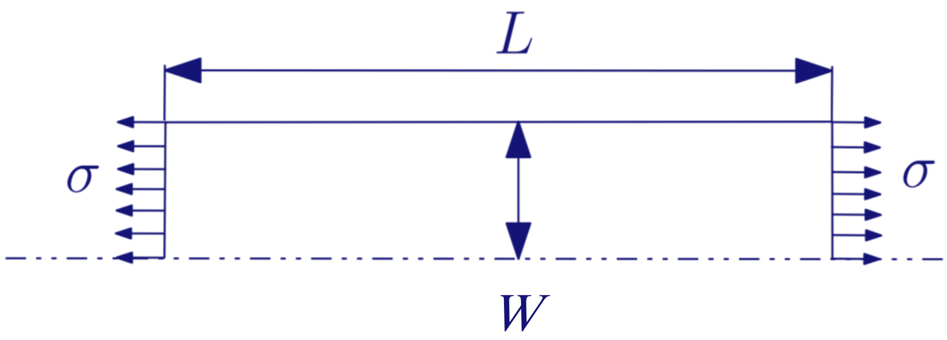

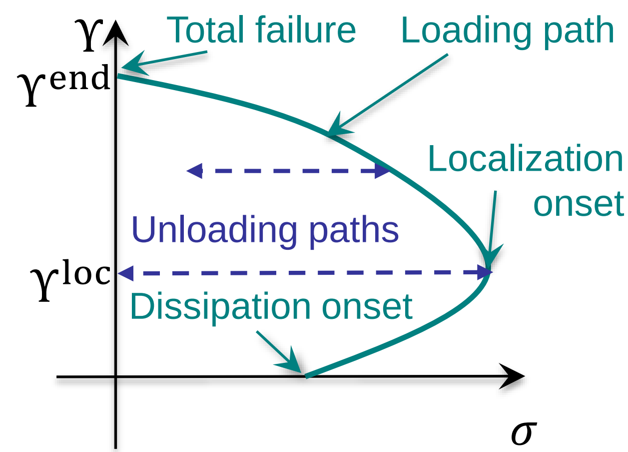

$$G_c = \frac{\mathcal{D}_{V_0}^{end} - \mathcal{D}_{V_0}^{loc}}{A_0}$$

  - This optimization problem allows to identify the damage model parameters $(\tilde{\alpha}_{dam}, \tilde{\beta})$ of the new definition of the two-part function:

$$\dot{\tilde{D}}_0 = \tilde{\alpha}_{dam}(\tilde{p}_0 + \Delta\tilde{p}_0 - \tilde{p}_{Onset})^{\tilde{\beta}}\Delta\tilde{p}_0$$

  - Less than 1% difference between full field and homogenized Gc → Good representation of SVE behavior up to total failure